*International Journal of Microwave and Wireless Technologies*

**cambridge.org/mrf**

# Designs, developments, challenges, and fabrication materials for MIMO antennas with various 5G and 6G applications: a review

Karrar Shakir Muttair[1,2], Oras Ahmed Shareef[1,3] and Hazeem Baqir Taher[4]

[1]Department of Computer Engineering Techniques, Electrical Engineering Technical College, Middle Technical University, Baghdad, Iraq; [2]Nanotechnology and Advanced Materials Research Unit, Faculty of Engineering, University of Kufa, Najaf, Iraq; [3]Department of Medical Devices Technical Engineering, Al-Ayen Iraqi University, AUIQ, Thi-Qar, Iraq and [4]Department of Computer Science, College of Education for Pure Sciences, Thi-Qar University, Thi-Qar, Iraq

**Cite this article:** Muttair KS, Shareef OA, Taher HB (2024) Designs, developments, challenges, and fabrication materials for MIMO antennas with various 5G and 6G applications: a review. *International Journal of Microwave and Wireless Technologies*, 1–30. https://doi.org/10.1017/S1759078724001004

Received: 14 March 2024
Revised: 2 September 2024
Accepted: 15 September 2024

**Keywords:**
5G and 6G technologies; 5G communication systems; 6G challenges; antenna designs; fabrication materials; isolation techniques; mmWaves MIMO antennas; single-input and single-output antennas; UWB MIMO antennas

**Corresponding author:** Karrar Shakir Muttair; Email: karrars.alnomani@uokufa.edu.iq

## Abstract

The rapid expansion of digital media platforms and their growing user base in the wireless industry necessitate communication systems to provide information at high speeds with reliable connections. Therefore, wireless communication systems with a single antenna cannot accomplish these requirements. Consequently, the access and utilization of multi-input multi-output (MIMO) antennas are becoming more common in contemporary high-speed transmission systems. This article covers the fundamentals of MIMO antenna operation, the metrics for MIMO antenna performance parameters, and the design methodologies for specifying the three most commonly used antennas (two-port, quad-port, and eight-port). Additionally, it discusses their ability to improve channel capacity significantly. It focuses on designing MIMO antennas with ultra-wideband (UWB) for 5G systems operating between 1 and 27 GHz and millimeter-wave (mmWave) bands from 30 to 100 GHz. This article is valuable for researchers interested in developing MIMO antennas for diverse applications. It compiles advanced methods related to materials, advancements, challenges, and state-of-the-art technologies used in the design of high-performance MIMO antennas. We concluded that antennas that operate at mmWave frequencies have small dimensions and suffer from isolation problems in the MIMO formation. In contrast, antennas operating below 6 GHz are large and do not suffer from isolation problems.

## Introduction

As technology has advanced to meet expectations, there have been requests for high-speed internet, high-definition video streaming, and fast data transfer rates [1, 2]. In addition, the widespread use of internet-based services has increased the demand for wireless communications systems with high rates of data and sufficient channel bandwidth. In most cases, single-input and single-output antennas cannot meet these demands [3]. Although these antennas are known as microstrips, they are extensively utilized and have several advantages, the most prominent of which are their low cost, suitable shapes, lightweight design, and flexibility via hybrid and monolith microwave circuits [4]. As a result, multi-input–multi-output (MIMO)-manufactured antennas, a new antenna approach, have become a viable choice for fast-speed technology for communication [5]. These antennas use coplanar shapes or strip lines to feed multiple radiating components individually to transmit and receive data [6, 7].

5G promises to enable large-scale events with thousands of users in smart cities, residences, healthcare, transportation, and infrastructure [8]. A 5G network utilizes low-, mid-, and high-frequency bands, enabling antennas to support multiple bands, handle wide bands, and adapt to various use cases for great coverage and connection [9, 10]. To support high data rates and accommodate large user counts, the deployment of multiband MIMO systems is expected. The fields of augmented reality, artificial intelligence, the Internet of Things, and three-dimensional media are examples of new technologies that are rapidly advancing communication. Because these technologies demand faster data rates, a rapid transition from 5G to 6G communications will be essential [11]. 6G wireless communication mostly uses the 0.1–10 THz frequencies [11]. The primary benefits that 6G offers to wireless manufacturing, healthcare, self-driving vehicles, intelligent cities, and renewable energy systems include larger capacity, more security, wider coverage, and very little latency [12].

In addition, these applications incorporate Wi-Fi (wireless fidelity), Bluetooth, global positioning system technology, wireless local area network, and other technologies to achieve a tiny


**Figure 1.** Frequency bands assigned to 5G and 6G wireless technologies.

multipurpose antenna [13]. The advent of 5G and 6G networks has sparked a wave of groundbreaking ideas put forth by researchers and rigorously evaluated [14]. As shown in Fig. 1, multiband MIMO permits the use of numerous frequency bands concurrently to cover the intended applications with decreased size and interference. These versatile antennas are perfect for wireless systems, offering a broader frequency range [15]. While working over many bands might raise the danger of interference across various frequency bands, needing careful design of the antenna and integration considerations, multiband antennas enable more effective use of the available spectrum of frequencies. The literature predominantly discusses wideband antennas and their effectiveness in 5G. However, there is a lack of characterization for multiband MIMO antennas in 5G and 6G [16]. Moreover, the 3rd Generation Partnership Project debuted 5G-Advanced in Release 18, laying the groundwork for its future evolution. Release 19 will concentrate on commercial deployment requirements and prepare for 6G [17].

The review in this paper is a study that categorizes several MIMO antenna designs and their properties. This study mainly concentrates on MIMO antenna design strategies using particular methodologies to obtain the necessary antenna efficiency. Additionally, the comparison tables included in the paper will assist readers in putting the approaches presented for improved MIMO antenna performance into practice and modifying them as necessary. Moreover, this review can offer a better understanding of future research directions.

This article presents six sections, organized as follows: The "Introduction" section provides a general introduction to MIMO antennas. The "Basic parameters of MIMO antennas" section introduces the criteria and parameters that determine the performance and efficiency of multiport MIMO antennas. The "Design categories for MIMO antennas" section presents and discusses the latest work related to the designs of MIMO antennas for frequencies from 1 to 27 GHz and those based on millimeter-wave (mmWave) frequencies. The "Importance of equivalent circuits for antennas" section discusses the importance of equivalent circuits for antennas. The "Challenges, developments, and future directions discussion" section discusses challenges, trends, and future developments in the fabrication and design of multiport MIMO antennas. Finally, the "Conclusions" section presents conclusions and suggestions for future MIMO antenna fabrication challenges.

## Basic parameters of MIMO antennas

In addition to the S-parameter and the radiation features, various diversity parameters are employed to verify the overall performance of a MIMO antenna. For real-world scenarios, MIMO antennas must adhere to predetermined diversity parameters. As a result, this section provides some fundamental diversity parameters for MIMO antennas.

### Envelope correlation coefficient *($\rho_{ECC}$)*

The diversity measure that shows how the neighboring MIMO antenna components correlate is ($\varepsilon_r$. It may be estimated using the S-parameters or radiation patterns. It's essential to evaluate its value using the far-range radiation pattern, as $\rho_{ECC}$ explains the unique radiation patterns of different radiating parts in MIMO systems. Additionally, it is evident that the majority of planar antennas experience loss. It's best to avoid using the S-parameters to calculate $\rho_{ECC}$. The allowable limit of envelope correlation coefficient (ECC) in a realistic situation must be less than 0.5. Equations (1) and (2) provide the formulas for utilizing information about the radiation pattern of a MIMO system. In contrast, Equation (3) provides the formula for $\rho_{ECC}$ utilizing information about the S-parameters [18, 19].

$$\rho_{ECC} = \frac{|a|^2}{a \times a} \tag{1}$$

$$a = \int_0^{2\Pi}\int_0^{\Pi} \left( \varrho^*_{\theta p}\varrho_{\theta q}P_\theta X_{PR} + \varrho^*_{\varphi p}\varrho_{\varphi q}P_\varphi \right) d\Omega \tag{2}$$

$$\rho_{ECC} = \frac{\left( \left| S_{(ii)}\, S_{(ij)} + S_{(ji)}\, S_{(jj)} \right|^2 \right)}{\left(1 - \left( \left|S_{(ii)}\right|^2 + \left|S_{(ji)}\right|^2 \right)\right)\left(1 - \left( \left|S_{(jj)}\right|^2 + \left|S_{(ij)}\right|^2 \right)\right)} \tag{3}$$

Where $X_{PR}$ is the cross-polarization level, it can be a percentage of the mean power across the φ & θ directions. *S* is the S-parameter (reflection coefficient) for each port at different frequencies, while *i* and *j* represent the number of ports in the MIMO array.

### Diversity gain (DG) ($G_{Diversity}$)

In wireless networks, $G_{Diversity}$ represents the quality and dependability of MIMO antennas. As a result, the $G_{Diversity}$ for the MIMO antenna within the permitted frequency spectrum has to be high (10 dB). Equation (4) can be utilized to calculate the $G_{Diversity}$ used the value of $\rho_{ECC}$ [20].

$$G_{Diversity} = 10 * \sqrt{1 - |\rho_{ECC}|^2} \tag{4}$$

### *Channel capacity loss (CCL)*

It denotes the volume of data that can be conveyed across a communication link, accounting for potential channel loss. A specified MIMO system's predetermined channel capacity loss (CCL) value is 0.4 bits/s/Hz. Equation (5) provides the formula for CCL through S-parameters [21].

$$CCL = -\log_2\left[ det \begin{bmatrix} 1 - \left[|S_{11}|^2 + |S_{12}|^2\right] & -\left[S^*_{11}S_{12} + S^*_{21}S_{12}\right] \\ -\left[S^*_{22}S_{21} + S^*_{12}S_{21}\right] & 1 - \left[|S_{22}|^2 + |S_{21}|^2\right] \end{bmatrix} \right] \tag{5}$$

### *Average effective gain (AEG)*

It is a crucial diversity parameter for MIMO antennas, indicating the additional power received compared to an isotropic antenna.

https://doi.org/10.1017/S1759078724001004 Published online by Cambridge University Press

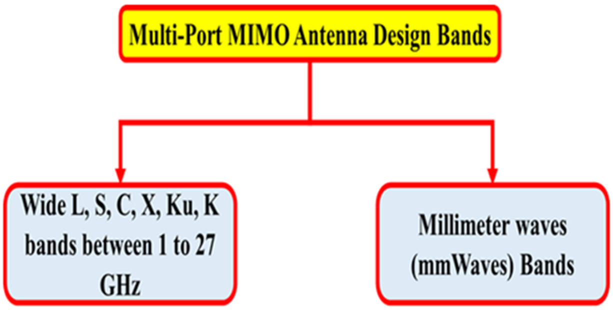


**Figure 2.** A schematic of multiband MIMO antenna designs.

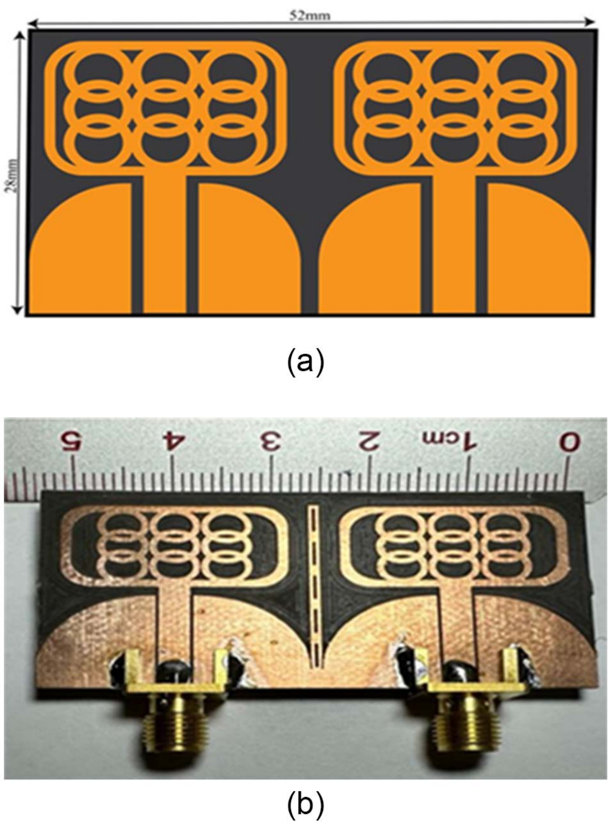


**Figure 3.** Antenna structural shapes on both sides: (a) simulation design; (b) realistic manufacturing design [23].

The average effective gain (AEG) ratio has to be <3 dB for a MIMO antenna to function better at equal power output. Using Eq. (6), the evaluation value of AEG can be determined [21].

$$AEG = \frac{AEG_i}{AEG_j} = \frac{0.5 \times \left[1 - |S_{ii}|^2 - |S_{ij}|^2\right]}{0.5 \times \left[1 - |S_{ij}|^2 - |S_{jj}|^2\right]} \tag{6}$$

### *Overall active reflection coefficient (OARC)*

The overall active reflection coefficient (OARC) of a MIMO system is calculated by dividing the total reflected power by the total incident power. The ratio of the total power incident upon the patch is compared to the total reflecting power resulting from the radiating components. Equation (7) provides the equation for the expanded

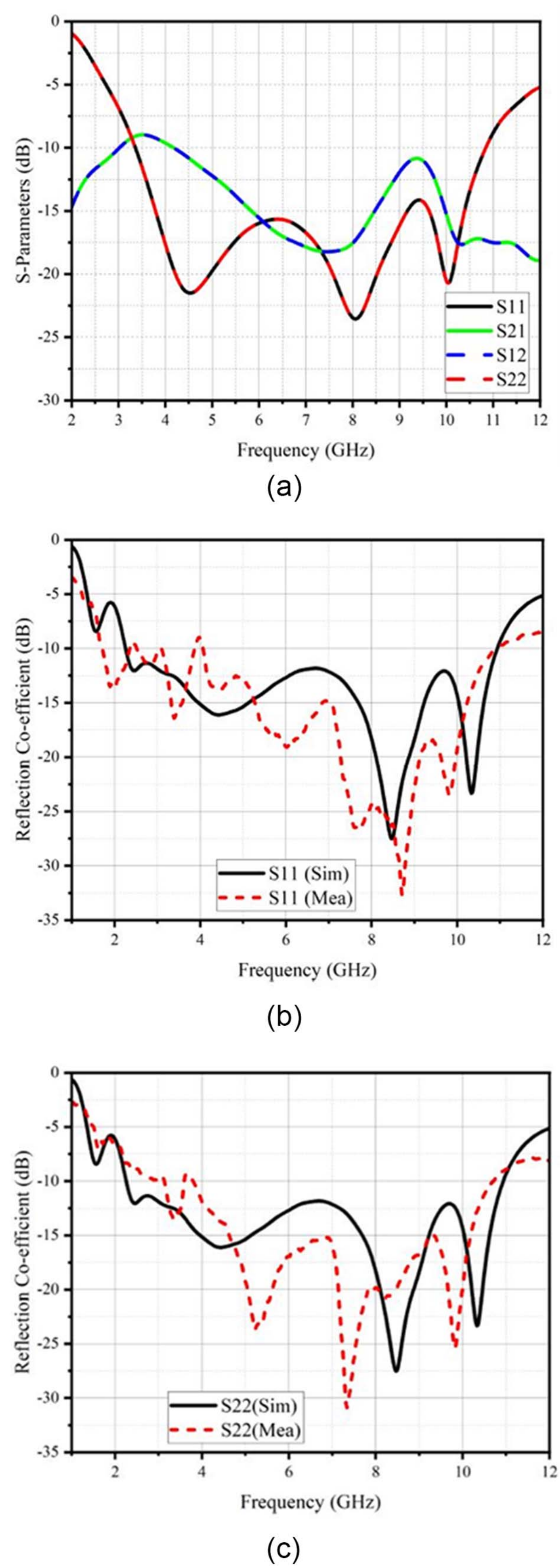


**Figure 4.** The reflection coefficient parameter of the antenna in simulation and realistic measurements. (a) The simulation side; (b) The simulation and practical side of S11; (c) The simulation and practical side of S22 [23].

https://doi.org/10.1017/S1759078724001004 Published online by Cambridge University Press

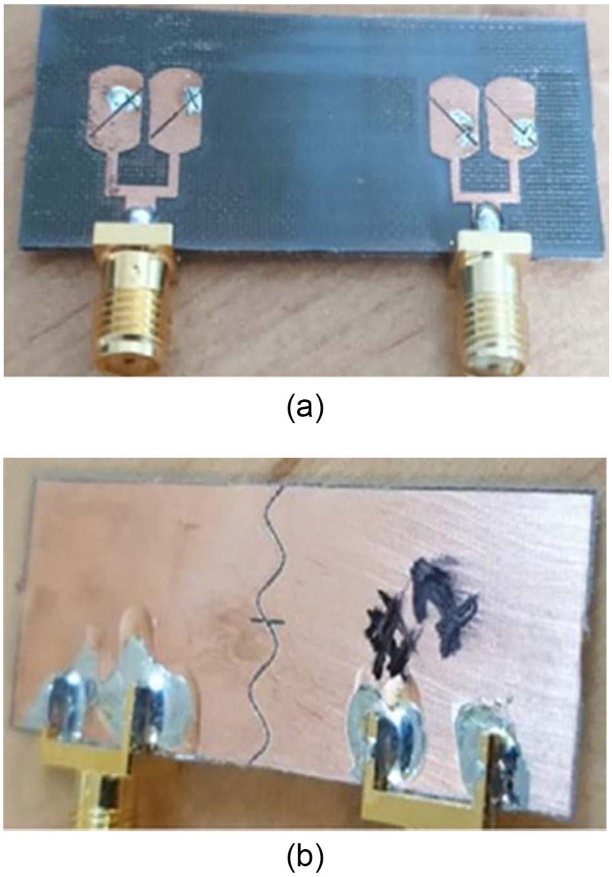


**Figure 5.** The fabrication geometry of the proposed antenna is (a) front view and (b) back view [24].

OARC for multi-port MIMO antennas. If we want to calculate the OARC for two ports, it will be according to the formula shown in Eq. (8) [22].

$$OARC = \frac{\sqrt{\sum_{i=1}^{N} |b_i|^2}}{\sqrt{\sum_{i=1}^{N} |a_i|^2}} \tag{7}$$

$$OARC = \frac{\sqrt{|S_{11} + S_{12}e^{j\theta}|^2 + |S_{21} + S_{22}e^{j\theta}|^2}}{\sqrt{2}} \tag{8}$$

Where $a_i$ and $b_i$ represent the coefficients of the scattering matrices, and is the number of ports in the MIMO configuration.

## Design categories for MIMO antennas

In this section, there are three subsections. The first discusses contemporary designs of dual-port MIMO antennas based on the ultra-wideband (UWB) band, covering frequencies from 1 to 27 GHz, including the L, S, C, X, Ku, and K bands. In addition to those based on mmWave frequencies of 28 GHz and above, as shown in Fig. 2. The second subsection discusses recent studies of quad-port antenna designs. The third subsection presents and discusses proposed works for antenna designs of eight ports and above.

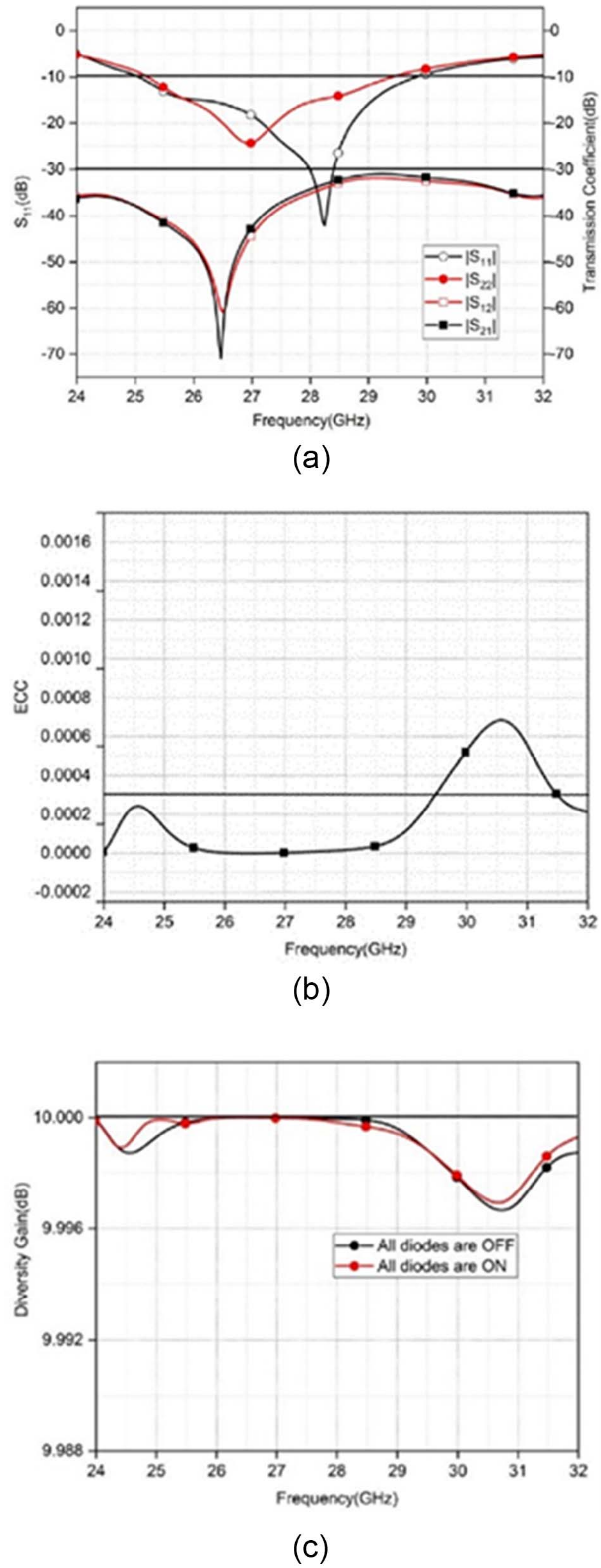


**Figure 6.** The antenna performance curves for (a) reflection coefficient (S11 and S22) and isolation (S12 and S21), (b) ECC, and (c) DG [24].

### *Dual-port MIMO antenna designs for various applications*

In a recent study [23], researchers proposed the design of a two-port compact antenna with its middle layer (substrate) made of

https://doi.org/10.1017/S1759078724001004 Published online by Cambridge University Press

**Table 1.** An overview of the latest research into the advancement of wideband two-port antennas

| Ref. | Year | Antenna dimensions ($W \times L \times H$) | No. ports | Prototype | Fabrication materials | Antenna operating frequency (GHz) | Bandwidth (GHz) | Max. gain (dBi) | Efficiency (%) | Max. isolation ratio (dB) | ECC | DG (dB) | CCL (bits/s/Hz) |
|---|---|---|---|---|---|---|---|---|---|---|---|---|---|
| [23] | 2023 | 52 × 28 × 0.787 | 2 |  | • Copper<br>• Rogers<br>5880 ($\varepsilon_r = 2.3$ and δ = 0.0009) | 2.3–11.5 | 9.2 | 5.9 | 85 | −16 | < 0.05 | 9.9 | NA* |
| [27] | 2023 | 60 × 60 × 0.8 | 2 |  | • Copper<br>• FR4<br>($\varepsilon_r = 4.3$ and δ = 0.025) | 1.67–2.28<br>2.39–2.79<br>3.13–3.74<br>4.69–5.34 | 0.61<br>0.4<br>0.61<br>0.65 | 5.60, 3.38, 3.78, 4.41 | 80 | −44 | < 0.1 | NA* | NA* |
| [28] | 2023 | 16 × 28 × 1.6 | 2 | 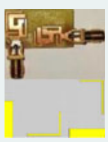 | • Copper<br>• FR4<br>($\varepsilon_r = 4.3$ and δ = 0.025) | 3.4–3.6<br>5.1–5.7<br>6–7 | 0.2<br>0.6<br>1 | 3.49 | 80 | −43 | < 0.04 | 9.5 | < 0.4 |
| [29] | 2024 | 87 × 60 × 1.6 | 2 | 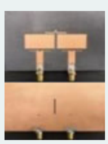 | • Copper<br>• F4B<br>($\varepsilon_r = 2.2$ and δ = 0.001) | 5.1–6.1 | 1 | 7.36 | NA* | −17 | < 0.03 | 9.15 | NA* |
| [30] | 2023 | 60× 60 × 1.6 | 2 | 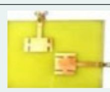 | • Copper<br>• Rogers<br>5880 | 7.28–12 | 4.72 | 4.6 | NA* | −39 | < 0.04 | 9.9 | < 0.25 |
| [31] | 2023 | 30 × 20 × 1.6 | 2 |  | • Copper<br>• FR4<br>($\varepsilon_r = 4.3$ and δ = 0.025) | 3.01–12.34 | 9.5 | 5.5 | 70 | −48 | < 0.0025 | 9.9 | 0.15 |
| [32] | 2023 | 44 × 82 × 1.6 | 2 | 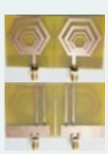 | • Copper<br>• FR4<br>($\varepsilon_r = 4.4$ and δ = 0.023) | 2.5–8 | 5.5 | 3.23 | NA* | −56 | < 0.004 | 9.96 | < 0.4 |
| [33] | 2023 | 40 × 40 × 1.5748 | 2 |  | • Copper<br>• FR4<br>($\varepsilon_r = 4.3$ and δ = 0.025) | 1.922–2.009<br>4.849–5.249 | 0.0870.4 | 7.17 | 84.75 | −54 | < 0.02 | 9.8 | < 0.5 |
| [25] | 2023 | 80 × 45 × 1.52 | 2 | 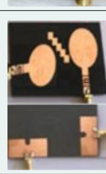 | • Copper<br>• Rogers<br>5880 ($\varepsilon_r = 2.2$ and δ = 0.0009) | 7.4–7.75 | 0.35 | 6 | 85 | −65 | 0.00012 | 9.9 | NA* |
| [34] | 2023 | 70 × 40 × 1.6 | 2 | 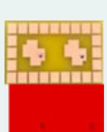 | • Copper<br>• FR4<br>($\varepsilon_r = 4.3$ and δ = 0.025) | 4.89–6.85 | 1.96 | 6.45 | 80 | −60 | < 0.002 | 9.9 | < 0.4 |

(*Continued*)

https://doi.org/10.1017/S1759078724001004 Published online by Cambridge University Press

**Table 1.** (*Continued.*)

| Ref. | Year | Antenna dimensions ($W \times L \times H$) | No. ports | Prototype | Fabrication materials | Antenna operating frequency (GHz) | Bandwidth (GHz) | Max. gain (dBi) | Efficiency (%) | Max. isolation ratio (dB) | ECC | DG (dB) | CCL (bits/s/Hz) |
|---|---|---|---|---|---|---|---|---|---|---|---|---|---|
| [35] | 2024 | 56 × 48 × 1.6 | 2 |  | • Copper<br>• FR4<br>($\varepsilon_r = 4.4$ and $\delta = 0.02$) | 2.24–2.41<br>5.1–5.3 | 0.17<br>0.2 | NA* | 50 | −46 | $<0.001$ | 9.99 | NA* |
| [36] | 2023 | 36 × 64 × 1.6 | 2 | 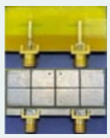 | • Copper<br>• FR4<br>($\varepsilon_r = 4.4$ and $\delta = 0.02$) | 3.7–4.3 | 0.6 | 4.1 | NA* | −40 | $<0.001$ | 9.99 | $<0.4$ |
| [37] | 2023 | 56 × 30 × 0.1 | 2 |  | • Copper<br>• Liquid<br>Crystal Polymer<br>($\varepsilon_r = 2.9$ and $\delta = 0.002$) | 3.5–4.5<br>8–18 | 1<br>10 | 6.2 | NA* | −59 | $<0.005$ | 9.99 | NA* |
| [38] | 2024 | 38 × 47.7 × 1.6 | 2 | 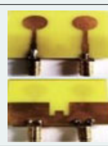 | • Copper<br>• FR4<br>($\varepsilon_r = 4.3$ and $\delta = 0.025$) | 2.83–7.21 | 4.38 | 4.8 | 92 | −34 | $<0.003$ | NA* | $<0.3$ |
| [39] | 2023 | 20 × 29 × 1.6 | 2 | 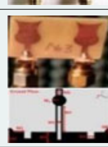 | • Copper<br>• FR4<br>($\varepsilon_r = 4.4$ and $\delta = 0.02$) | 5–13.5 | 8.4 | 5.5 | NA* | −40 | $<0.002$ | 9.9 | $<0.3$ |
| [40] | 2024 | 14 × 37 × 1.6 | 2 | 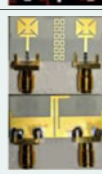 | • Copper<br>• Rogers<br>4003<br>$= 3.55$ and $\delta = 0.0027$) | 5.9–7.4 | 1.5 | 2.2 | 90 | −56 | $<0.001$ | NA* | NA* |
| [41] | 2023 | 56.4 × 36.6 × 1.524 | 2 | 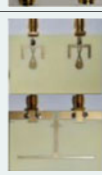 | • Copper<br>• Rogers<br>4003<br>($\varepsilon_r = 3.55$ and $\delta = 0.0027$) | 3.38–3.61<br>4.51–4.96<br>6.06–7.51 | 0.23<br>0.45<br>1.45 | 6 | 76 | −43 | $<0.2$ | NA* | NA* |
| [42] | 2023 | 120 × 60 × 0.8 | 2 | 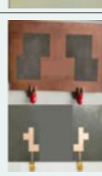 | • Copper<br>• Rogers<br>5880<br>($\varepsilon_r = 2.2$ and $\delta = 0.0009$) | 3–4.2 | 1.2 | 4 | NA* | −42 | $<0.005$ | 9.99 | $<0.5$ |
| [43] | 2023 | 40× 25 × 1.6 | 2 |  | • Copper<br>• FR4<br>($\varepsilon_r = 4.4$ and $\delta = 0.02$) | 3–6 | 3 | 3.6 | 85.3 | −60 | $<0.05$ | 9.8 | $<0.3$ |
| [44] | 2023 | 85 × 45 × 1.6 | 2 | 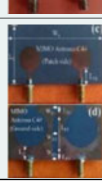 | • Copper<br>• Rogers<br>5880<br>$= 2.2$ and $\delta = 0.0009$) | 3–26 | 23 | 9.5 | 95.4 | −45 | $<0.02$ | 9.8 | $<0.4$ |

https://doi.org/10.1017/S1759078724001004 Published online by Cambridge University Press

**Table 2.** A detailed comparison and summary of recent research papers introducing dual-port antennas in the mmWave bands

| Ref. | Year | Antenna dimensions ($W \times L \times H$) $mm^3$ | No. ports | Prototype | Fabrication materials | Antenna operating frequency (GHz) | Bandwidth (GHz) | Max. gain (dBi) | Efficiency (%) | Max. isolation ratio (dB) | ECC | DG (dB) | CCL (bits/s/Hz) |
|---|---|---|---|---|---|---|---|---|---|---|---|---|---|
| [26] | 2023 | 55.27 × 27.635 × 1.62 | |  | • Copper<br>• FR4<br>($\varepsilon_r = 4.3$ and $\delta = 0.025$) | 27–40 | 13 | 10 | 65 and 90 | −65 | $<0.0001$ | 9.99 | $<0.4$ |
| [45] | 2023 | 30 × 30 × 1.6 | 2 | 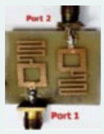 | • Copper<br>• FR4<br>($\varepsilon_r = 4.4$ and $\delta = 0.02$) | 19.82–27.31<br>31.07–35.83 | 7.4<br>4.7 | 5.8<br>5.2 | 78 | −48 | $<0.04$ | 9.98 | $<0.25$ |
| [46] | 2023 | 32 × 26 × 1 | 2 |  | • Copper<br>• FR4<br>($\varepsilon_r = 4.4$ and $\delta = 0.02$) | 1.98–30.8 | 28.82 | 10.4 | NA* | −46 | $<0.03$ | NA* | NA* |
| [47] | 2023 | 25 × 26 × 1.6 | 2 |  | • Copper<br>• Rogers<br>5880<br>($\varepsilon_r = 2.2$ and $\delta = 0.0009$) | 26–60 | 34 | 11.1 | 94 | −59 | $<0.0068$ | 9.967 | NA* |
| [48] | 2023 | 30 × 30 × 17.228 × 0.508 | 2 | 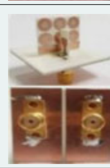 | • Copper<br>• Rogers<br>4003<br>$= 3.38$ and $\delta = 0.0027$) | 24–27 | 3 | 4.99 | NA* | −40 | NA* | NA* | NA* |
| [49] | 2023 | 20.5 × 12 × 0.79 | 2 |  | • Copper<br>• Roger<br>6002<br>$= 2.94$ and $\delta = 0.0012$) | 25.5–30 | 4.5 | 8.75 | 99 | −44 | NA* | NA* | NA* |
| [50] | 2023 | 35 × 35 × 1.6 | 2 |  | • Copper<br>• Rogers<br>5880<br>$= 2.2$ and $\delta = 0.009$) | 25–40 | 15 | 4.4 | 83 | −60 | 0.0016 | 9.99 | NA* |
| [51] | 2023 | 15 × 26 × 1.52<br>15 × 28.75 × 1.52 | 2<br>2 |  | • Copper<br>• Rogers<br>6002<br>($\varepsilon_r = 2.94$ and $\delta = 0.0012$) | 26–34.25<br>26–34.75 | 8.25<br>8.75 | 11.25 | $>91$ | −35<br>−43 | $<0.001$<br>$<0.0001$ | $>9.8$<br>$>9.99$ | $<0.025$<br>$<0.001$ |
| [52] | 2023 | 10 × 28 × 0.787 | 2 |  | • Copper<br>• Rogers<br>5880<br>$= 2.2$ and $\delta = 0.0009$) | 26.5–27.1<br>39.15–40.69 | 0.6<br>1.54 | 7.29<br>7.45 | 90.9<br>94.5 | −43 | $<0.03$ | 9.99 | $<0.35$ |
| [53] | 2023 | 44 × 28.22 × 1.6 | 2 | 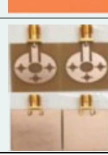 | • Copper<br>• FR4<br>($\varepsilon_r = 4.4$ and $\delta = 0.02$) | 8–11.1<br>16–16.5<br>17.9–28 | 3.1<br>0.5<br>10.1 | 8.46 | 73 | −40 | $<0.004$ | $>9.99$ | NA* |

(*Continued*)

https://doi.org/10.1017/S1759078724001004 Published online by Cambridge University Press

**Table 2.** (*Continued.*)

| Ref. | Year | Antenna dimensions ($W \times L \times H$) $mm^3$ | No. ports | Prototype | Fabrication materials | Antenna operating frequency (GHz) | Bandwidth (GHz) | Max. gain (dBi) | Efficiency (%) | Max. isolation ratio (dB) | ECC | DG (dB) | CCL (bits/s/Hz) |
|---|---|---|---|---|---|---|---|---|---|---|---|---|---|
| [54] | 2024 | 16 × 10 × 0.508 | 2 |  | • Copper<br>• Rogers<br>5880 ($\varepsilon_r$= 2.2 and $\delta = 0.0009$) | 27.2–29<br>34–40.2<br>47.5–51.3 | 1.8<br>6.2<br>3.8 | 11.2 | NA* | −50 | <0.002 | 9.99 | <0.25 |
| [55] | 2023 | 15 × 15 × 0.508 | 2 |  | • Copper<br>• Rogers<br>5880 ($\varepsilon_r = 2.2$ and $\delta = 0.0009$) | 22–24.5 | 2.5 | 7.28 | 95 | −47 | <0.05 | 9.99 | <0.5 |
| [56] | 2023 | 26 × 19.2 × 1.6 | 2 | 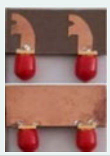 | • Copper<br>• Rogers<br>5880 ($\varepsilon_r = 2.2$ and $\delta = 0.0009$) | 20–40 | 20 | 8.17 | >85 | −55 | <0.0001 | NA* | NA* |
| [57] | 2023 | 38 × 18 × 0.8 | 2 |  | • Copper<br>• Rogers<br>5880 ($\varepsilon_r = 2.2$ and $\delta = 0.0009$) | 27–29 | 2 | 8.75 | 93.5 | −55 | <0.005 | >9.9 | NA* |
| [58] | 2023 | 190.46 × 56.65 × 0.254 | 2 |  | • Copper<br>• Rogers<br>5880 ($\varepsilon_r = 2.2$ and $\delta = 0.0009$) | 38.28–39.9 | 1.62 | 25.75 | 90 | −60 | <0.022 | >9.89 | NA* |
| [59] | 2023 | 30 × 15 × 0.203 | 2 |  | • Coppe<br>• Rogers<br>4003 ($\varepsilon_r = 3.55$ and $\delta = 0.0021$) | 25.5–30.5<br>35.5–40 | 5<br>4.5 | 5.7 6.9 | NA* | −41 | <0.0002 | 9.99 | <0.3 |
| [60] | 2023 | 75 × 45 × 1 | 2 |  | • Copper<br>• Rogers<br>5880 ($\varepsilon_r = 2.2$ and $\delta = 0.0009$) | 2. 13–30 | 27.87 | 4–7 | NA* | −54 | <0.02 | >9.99 | <0.45 |
| [61] | 2023 | 19 × 12 × 0.508 | 2 |  | • Copper<br>• Rogers<br>5870 ($\varepsilon_r = 2.33$ and $\delta = 0.0012$) | 30–41 | 11 | 9.5 | 96 | −51 | <0.005 | >9.6 | NA* |
| [62] | 2023 | 30 × 15 × 0.9 | 2 |  | • Copper<br>• Rogers<br>5880 ($\varepsilon_r = 2.2$ and $\delta = 0.0009$) | 26.69–29.55<br>38.24–42.53 | 2.86<br>4.29 | 5.4 | >84 | −56 | <0.03 | 9.99 | <0.36 |
| [63] | 2024 | 18 × 9.2 × 0.787 | 2 | 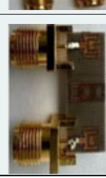 | • Copper<br>• Rogers<br>5880 ($\varepsilon_r = 2.2$ and $\delta = 0.0009$) | 24–28.8<br>36.6–40.8 | 4.8<br>4.2 | 6<br>7.8 | NA* | −40 | <0.0001 | 9.99 | <0.5 |

(*Continued*)

https://doi.org/10.1017/S1759078724001004 Published online by Cambridge University Press

**Table 2.** (*Continued.*)

| Ref. | Year | Antenna dimensions ($W \times L \times H$) $mm^3$ | No. ports | Prototype | Fabrication materials | Antenna operating frequency (GHz) | Bandwidth (GHz) | Max. gain (dBi) | Efficiency (%) | Max. isolation ratio (dB) | ECC | DG (dB) | CCL (bits/s/Hz) |
|---|---|---|---|---|---|---|---|---|---|---|---|---|---|
| [64] | 2022 | 14 × 20 × 0.168 | 2 | 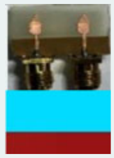 | • Copper<br>• Roger 4350B ($\varepsilon_r = 3.48$ and $\delta = 0.0037$) | 16.7–25.4 | 8.7 | 5.34 | 80 | −32 | <0.16 | 9.9 | <0.41 |
| [65] | 2022 | 27.65 × 12 × 0.273 | 2 |  | • Copper<br>• Rogers 4003 ($\varepsilon_r = 3.55$ and $\delta = 0.0027$) | 27.5–29.4<br>36.4–41.9 | 1.9<br>5.5 | 5.2<br>5.3 | NA* | −44 | <0.0001 | 9.99 | <0.4 |

RO5880, which has a thickness of 0.787 mm. The overall dimensions of this antenna are 52 × 28 $mm^2$, as shown in Figs. 3(a) and (b). This antenna is designed for operation in a resonant frequency range of 2.3–11.5 GHz, as shown in Figs. 4(a), (b) and (c), making it suitable for UWB applications. The suggested antenna shows significant isolation improvement, reaching up to −16 dB, as shown in Fig. 4(a), achieved using shared radiators with small rectangular slots. This feature reduces interference, boosts overall performance, and demonstrates its capabilities through a detailed analysis of MIMO performance factors in Table 1. A good range of results was identified. The simulations and measurements indicate that the antenna design is feasible and successful. Its broad bandwidth, small size, and improved isolation qualities make it an attractive option for UWB imaging with microwave systems of the future.

In addition, the authors presented a two-element MIMO antenna that operates at mmWave frequencies (25.2–29.5 GHz). This antenna is characterized by its rectangular outer shape, as shown in Figs. 5(a) and (b), with geometric dimensions ($W = 50$ mm, $L = 12$ mm, $H = 0.787$ mm). The material used for its substrate layer is Rogers 5880, which has a permittivity ($\varepsilon_r = 2.2$) and loss tangent ($\delta = 0.02$). The authors clarified that the antenna resonates at 28.4 GHz and that the isolation ratio between the first and second ports is lower than −32 dB, as demonstrated in Fig. 6(a). They added that because the antenna offers acceptable performance parameters, it is appropriate for communications systems based on mmWave frequencies. For example, the gain rate reached 11.4 dBi, the ECC is <0.00025, and the diversity gain (DG) is >9.996 dB, as shown in Figs. 6(b) and (c), respectively [24].

Other scholars have recently published numerous studies on the design of two-port MIMO antennas, which are well detailed in Table 1. Table 1 showcases the comparative data of diverse antenna designs tailored for various purposes. Because mutual coupling is crucial in MIMO antennas, researchers in reference [25] found that MIMO elements have a notable isolation ratio of −65 dB. Although the remaining designs were satisfactory and produced similar results, one stood out above the others.

The remaining recent works have been compiled in Table 2 using the same methodology. Researchers present a dual-port MIMO antenna operating in mmWave bands. It has been discovered that a significant number of the designs utilized similar materials to fabricate the antennas. In addition, there is a discrepancy in the results: the researchers in reference [26] achieved good results for isolation ratio, efficiency, ECC, DG, CCL, and gain. While the other proposed designs also produced good results, they showed varied performance due to the different dimensions and geometries suggested by each author for the antenna design.

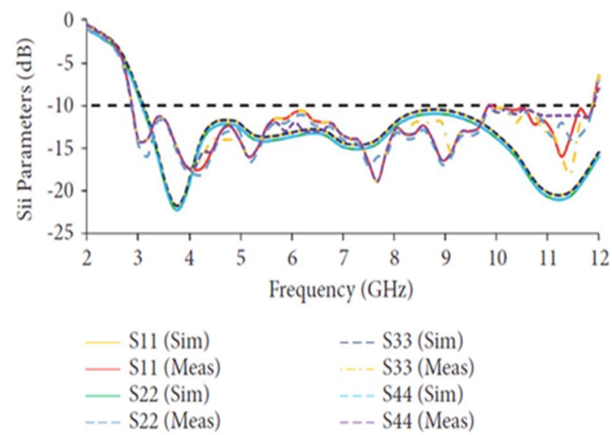


**Figure 7.** The S-parameter curves versus the different frequencies [66].

## Four-port MIMO antenna designs for various applications

Recently, researchers presented in reference [66] a foldable MIMO antenna for smart apparel applications with UWB capability. The MIMO antenna operated in the 2.9–12 GHz band, as shown in Fig. 7, and consisted of four octagonal radiators with empty holes built into them, as shown in Figs. 8(a), (b) and (c). The dimensions and thickness of this antenna are 50 × 50 × 1.6 $mm^3$. The antenna's radiation and diversification performances are analyzed, and the metrics obtained include ECC < 0.045, DG > 9.9 dB, OARC < − 14 dB, and CCL < 0.13 bits/s/Hz. Additionally, the suggested antenna has a 20 mm bend radius, making it appropriate for applications in wearable devices. This antenna is suitable for applications involving patient monitoring.

In another recent work in reference [67], a compact UWB four-element MIMO antenna design with band rejection is presented, as shown in Figs. 9(a) and (b). The recommended antenna can function at 3–12 GHz and has S11 ≤ −10 dB thanks to the four components' rectangle radiators with curving sides and partially grounded planes with an engraved slot. The antennas were

https://doi.org/10.1017/S1759078724001004 Published online by Cambridge University Press


**Figure 8.** (a) Prototype antenna with four ports on the front; (b) antenna bending model at 20 mm; and (c) antenna performance measurement using a vector network analyzer device [66].

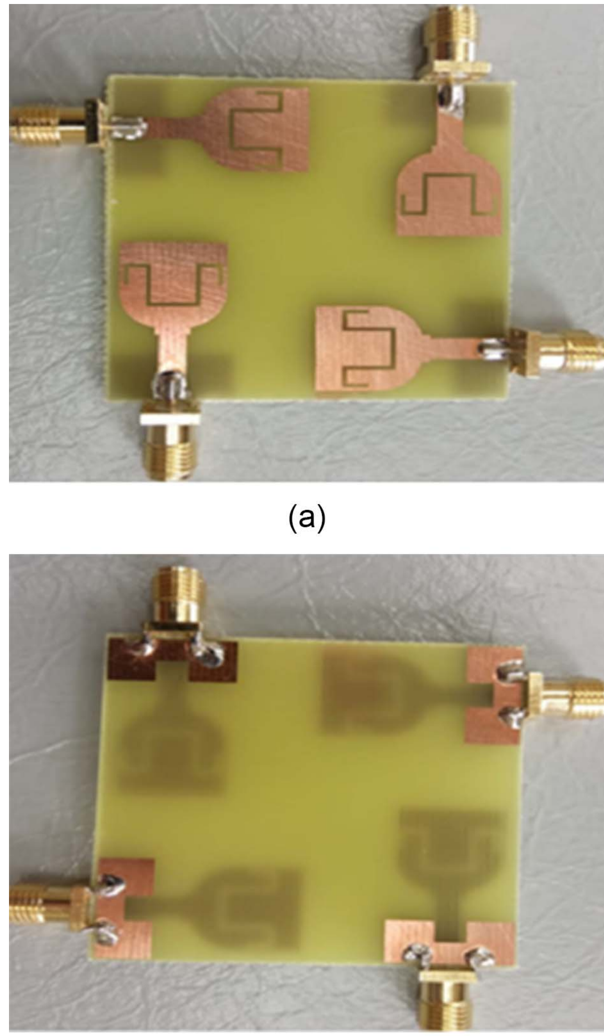


**Figure 9.** An antenna manufacturing prototype (a) on the front side and (b) on the back side [67].

arranged orthogonally without decoupling features, simplifying the engineering process and ensuring high isolation between the components. On a cheap FR4 substrate, the recommended design dimension and thickness are $47 \times 47 \times 1.6\text{mm}^3$. The antenna operates within the operational bands with a maximum gain of 4.8 dBi, as shown in Fig. 10(a). It has an ECC of less than 0.005, as shown in Fig. 10(b). The antenna has a DG of 9.98 dB, as shown in Fig. 10(c). The CCL of the antenna is less than 0.4 bit/s/Hz, as shown in Fig. 10(d). The results were consistently positive, which allowed the recommended antenna to be employed in UWB MIMO communications systems.

A recent research article [68] presented a quad-port broadband metamaterial (MM) antenna to achieve a high gain in new radio communications operating at sub-6 GHz, as shown in Figs. 11(a) and (b). The suggested four MIMO antennas are arranged orthogonally to the neighboring antennas. It achieves the compact size and properties of 55.2% bandwidth with a low interelement edge-to-edge length of 0.19 $\lambda_{min}$ at 3.25 GHz. The intended MIMO system is implemented using an inexpensive FR-4 printed material, measuring just 0.65 $\lambda_{min}$×0.65 $\lambda_{min}$×0.14 $\lambda_{min}$, as shown in Figs. 12(a), (b) and (c). A high peak output gain of about 7.1 dBi

https://doi.org/10.1017/S1759078724001004 Published online by Cambridge University Press

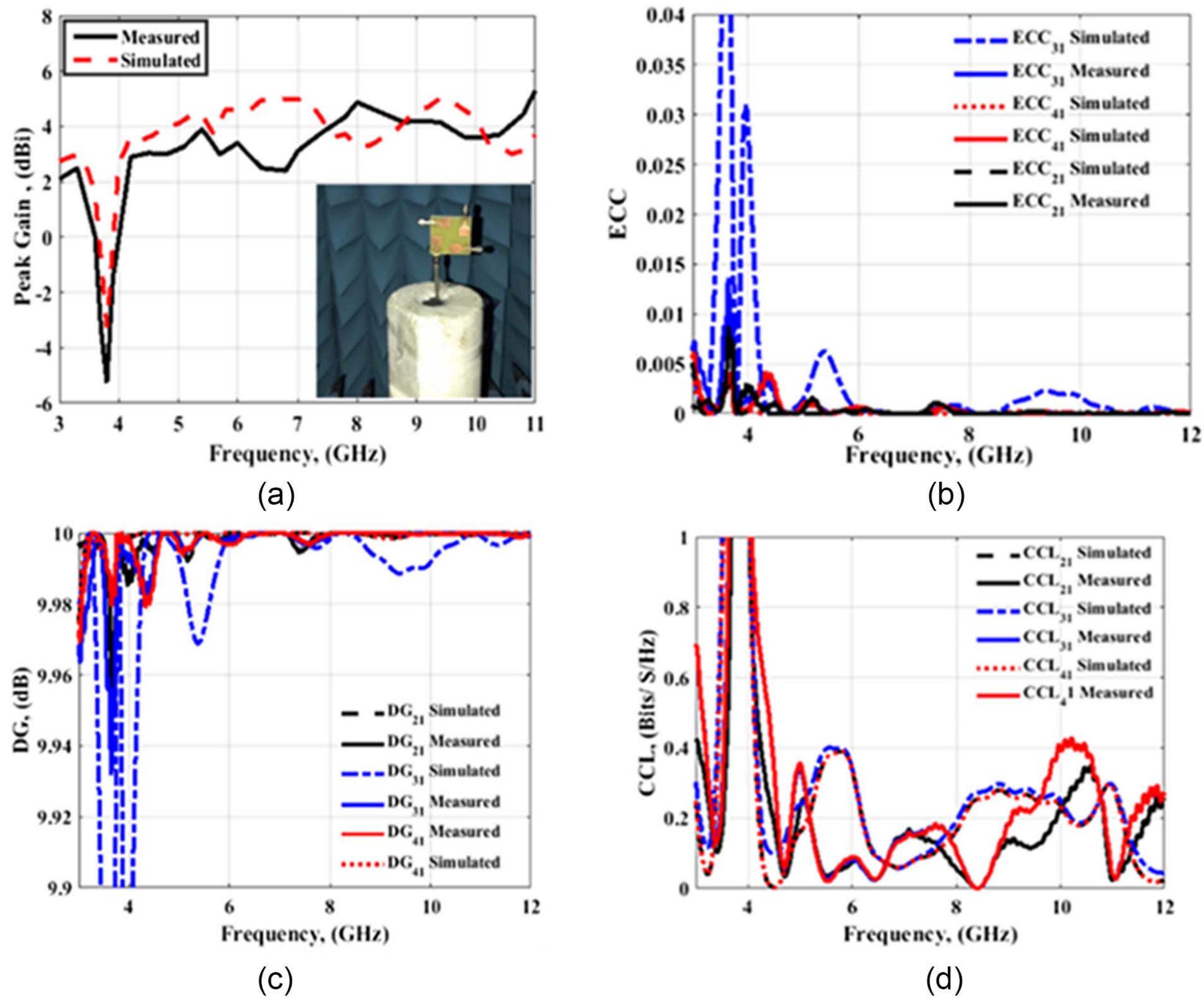


**Figure 10.** The basic parameters to determine the efficiency of the proposed antenna in reference [67] are (a) gain curves, (b) ECC curves, (c) DG curves, and (d) CCL curves.

between −9 and −50 dB isolation is displayed by the developed miniature MIMO system with an MM reflector, as shown in Fig. 11(a). Furthermore, the proposed broad-spectrum MM increases MIMO's various perspectives and radiation properties, with an average overall efficiency of 68% throughout the target bands. The specified antenna for the MIMO system has good multiplex efficiency, with a value of more than −1.4 dB, an acceptable CCL of less than 0.35b/s/Hz, an exemplary DG of 9.96 dB, and an exceptional ECC of less than 0.045. The values of the rest of the parameters that determine antenna performance are listed in Table 3. In the end, the researchers explained that the proposed antenna is a potential approach to the 5G system.

In another recent study [69], researchers proposed a four-port MIMO antenna with dimensions of 90 × 90 × 1.6 $mm^3$, as shown in Figs. 13(a), (b), (c) and (d). The researchers explained that the antenna is proposed for wide-band communications systems. Based on the results achieved by the antenna, it was good in most parameters to determine performance and efficiency. It worked in a wide frequency range that reached 9.33 GHz because the antenna operates at frequencies from 2.67 to 12 GHz, as shown in the reflection coefficient (return losses) curves in Fig. 14(a). In addition, it achieves an isolation ratio between ports of less than −15 dB, as shown in Fig. 14(b), an ECC of less than 0.1, and a DG of 9.97 dB. While the gain and efficiency for the antenna reached 5 dBi and 75%, respectively, the researchers concluded that the antenna is well-suited for UWB applications.

In addition, in a recent article [70], academics proposed manufacturing a four-port MIMO antenna, as shown in Figs. 15(a) and (b). This antenna is made of copper for both the patch and ground layers. While its substrate layer is made of FR4, the design dimensions of the antenna are 50 × 20. This antenna operates at two resonant frequencies: 38 and 60 GHz, as shown in Fig. 16(a). The proposers confirmed that the antenna is suitable for 5G system applications. The antenna provides satisfactory results for the isolation ratio between the four ports, which reached −42 dB at 38 GHz and −47 dB at 60 GHz (Fig. 16(b)). Moreover, the value of ECC is <0.05, and the DG is >9.98. The gain values reach 6.5 at 38 GHz and 5.5 dBi at 60 GHz.

Other recent articles summarize the designs of quad-port (2 × 2) MIMO antennas based on frequencies below 27 GHz in Table 3, while designs based on mmWave bands are listed in Table 4. It has been found that antennas operating at sub-6 GHz frequencies have larger dimensions and do not experience isolation problems between the ports. In contrast, mmWave antennas are small in dimensions and suffer from isolation problems between antenna elements in MIMO configuration.

https://doi.org/10.1017/S1759078724001004 Published online by Cambridge University Press

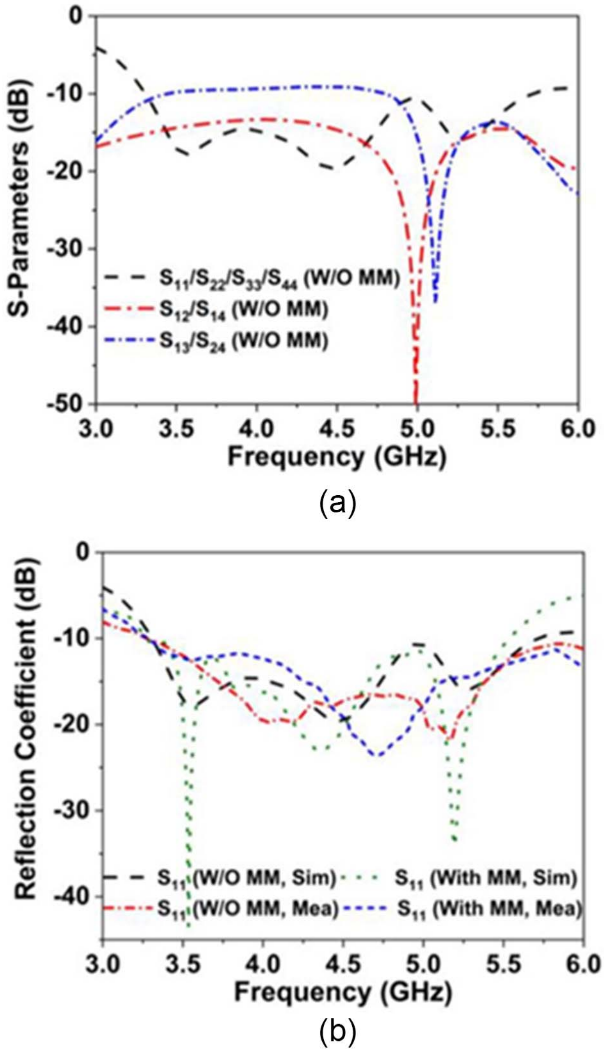


**Figure 11.** The return loss curves versus the various frequencies for (a) simulation side curves and (b) comparisons between simulation side curves and manufacturing measurements [68].

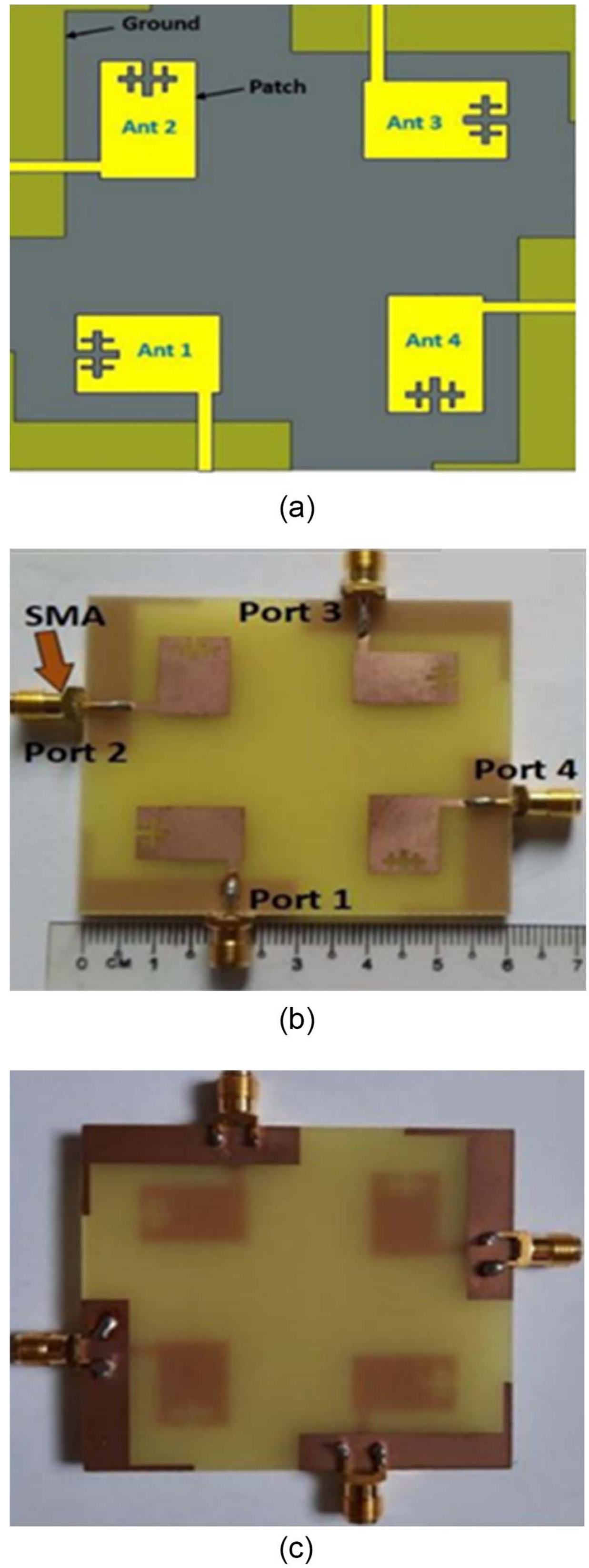


**Figure 12.** The design of the proposed antenna shapes (a) CST simulation, (b) practical design on the front side, and (c) practical design on the back side [68].

## *Six and more ports MIMO antenna designs for various applications*

In the recent manuscript [120], the researchers designed a multi-port antenna (six ports), as shown in Figs. 17(a) and (b). The researchers focused on providing this antenna to operate at mmWave frequencies, so the antenna worked in two bands, the first band from 27.7 to 28.1 GHz and the second band from 36.92 to 39.5 GHz, as shown in Figs. 18(a) and (b).

The researchers were able to obtain good results in light of the challenges in the field of antenna manufacturing. So, the antenna achieved satisfactory outputs for the isolation value that reached less than −20, as shown in Fig. 18(c). The highest gain value for the first band reached 13.3 dBi, and the second band reached 10.09 dBi, as shown in Fig. 19(a). While the ECC value is $<0.01$, the DG value is $>9.988$, and the CCL value was less than 0.4 bits/s/Hz. In the end, the antenna achieved an overall efficiency of 92% and 94% for the two bands, respectively, as shown in Fig. 19(b).

https://doi.org/10.1017/S1759078724001004 Published online by Cambridge University Press

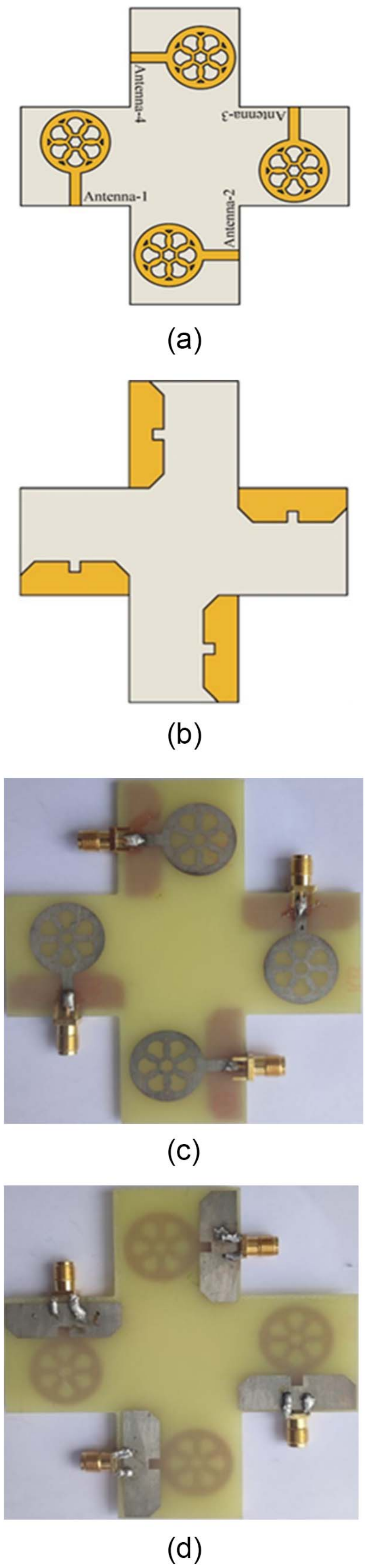


**Figure 13.** Antenna designs for simulation and manufacturing: (a) simulation front side, (b) simulation back side, (c) fabrication front side, and (d) fabrication back side [69].

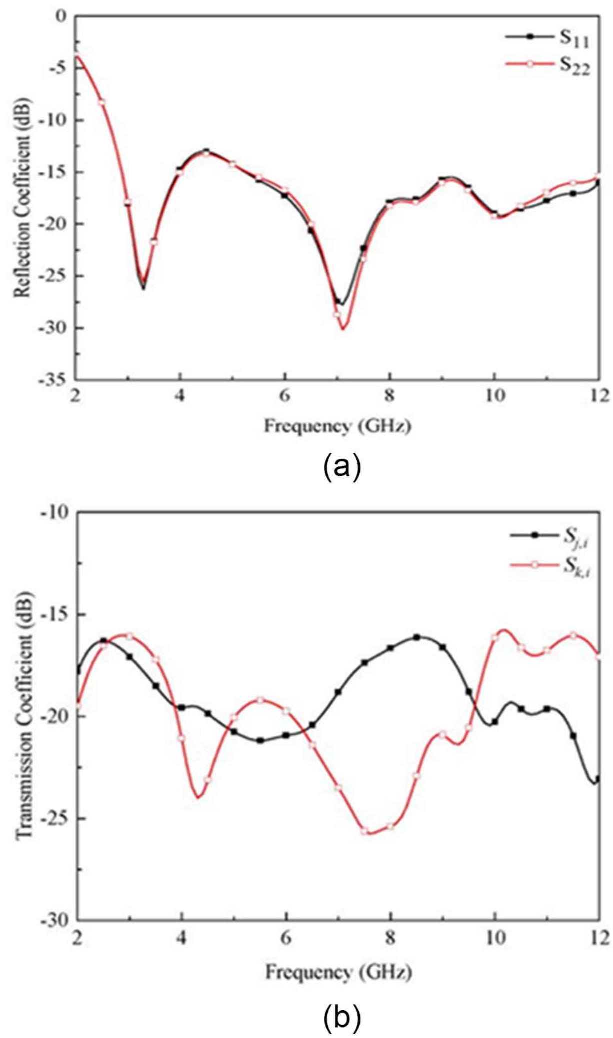


**Figure 14.** Curves of S-parameters versus different frequencies from 2 to 12 GHz (a) return loss curves and (b) isolation curves between ports [69].

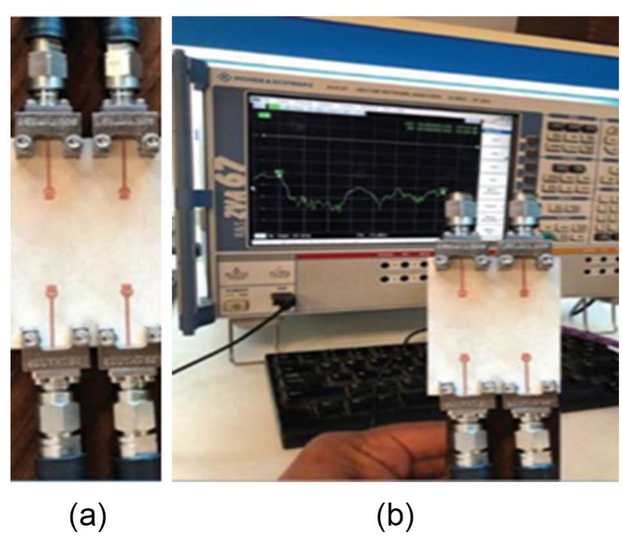


**Figure 15.** Practical aspects of the proposed antenna include (a) manufacturing the antenna and (b) measuring the antenna's performance using an analysis device (Rohde & Schwarz) [70].

https://doi.org/10.1017/S1759078724001004 Published online by Cambridge University Press

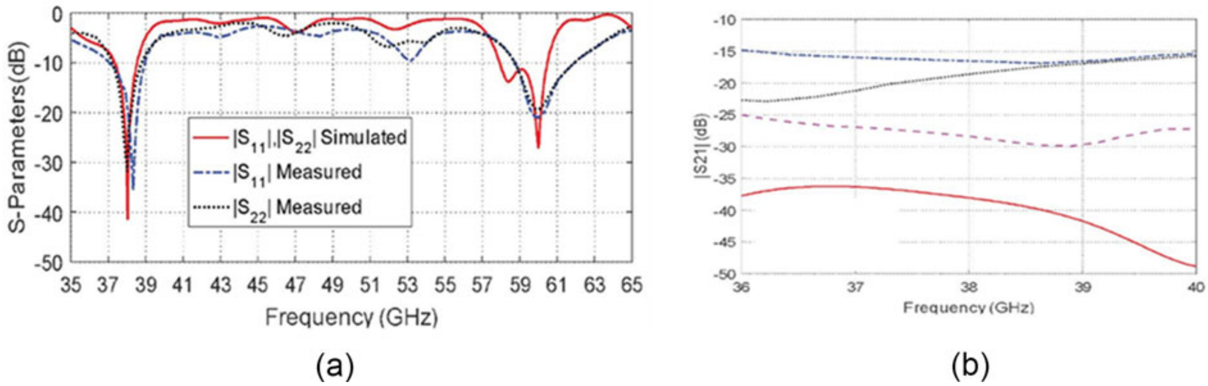


**Figure 16.** (a) S-parameter curves for the simulation and measurement sides, and (b) isolation curves between ports [70].

**Table 3.** A summary of recent studies on the design of a four-port antenna that operates at frequencies below 27 GHz

| Ref. | Year | Antenna dimensions (W × L × H) $mm^3$ | No. ports | Prototype | Fabrication materials | Antenna operating frequency (GHz) | Bandwidth (GHz) | Max. gain (dBi) | Efficiency (%) | Max. isolation ratio (dB) | ECC | DG (dB) | CCL (bits/s /Hz) |
|---|---|---|---|---|---|---|---|---|---|---|---|---|---|
| [71] | 2023 | 58 × 58 × 0.787 | 4 |  | • Copper<br>• Rogers 5880 ($\varepsilon_r = 2.2$ and $\delta = 0.0009$) | 4.4–14.4 | 10 | 5.3 | 86 | −59 | $<0.04$ | 9.9 | $<0.19$ |
| [72] | 2023 | 68 × 68 × 0.8 | 4 | 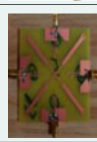 | • Copper<br>• FR4 ($\varepsilon_r = 4.4$ and $\delta = 0.02$) | 3.3–3.6<br>4.8–5.0 | 0.3<br>0.2 | 2.5<br>4.5 | 90 | −51 | $<0.0025$ | 9.99 | $<0.4$ |
| [68] | 2023 | 60 × 60 × 1.6 | 4 |  | • Copper<br>• FR4 ($\varepsilon_r = 4.3$ and $\delta = 0.025$) | 3 –6 | 3 | 7.1 | 71.5 | −35 | $<0.045$ | 9.96 | $<0.35$ |
| [73] | 2024 | 112.5 × 67.5 × 0.79 | 4 |  | • Copper<br>• Physical prototype (Arlon AD270) ($\varepsilon_r = 2.7$) | 5.6–6.3 | 0.7 | 9.6 | 90 | −60 | $<0.002$ | 9.99 | $<0.4$ |
| [74] | 2023 | 78 × 78 × 1.6 | 4 |  | • Copper<br>• Rogers 5880 ($\varepsilon_r = 2.2$ and $\delta = 0.0009$) | 2.1–3.2<br>3.9–4.6<br>5.4–7.4<br>7.7–9.4<br>9.6–11 | 1.1<br>0.7<br>2<br>1.7<br>1.4 | 6.6 | 85 | −50 | $<0.05$ | 9.8 | $<0.8$ |
| [75] | 2023 | 58 × 58 × 1.6 | 4 | 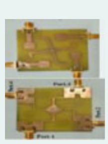 | • Copper<br>• FR4 ($\varepsilon_r = 4.3$ and $\delta = 0.025$) | 2.8–12.1 | 9.3 | 6.57 | 97 | −39 | $<0.003$ | 9.9 | $<0.4$ |
| [76] | 2023 | 80 × 80 × 0.508 | 4 | 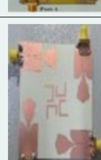 | • Copper<br>• Rogers 4003 ($\varepsilon_r = 3.55$ and $\delta = 0.0027$) | 4–21 | 12 | 7.38 | 85 | −55 | $<0.002$ | 9.9 | NA* |

(*Continued*)

https://doi.org/10.1017/S1759078724001004 Published online by Cambridge University Press

**Table 3.** (*Continued.*)

| Ref. | Year | Antenna dimensions (W × L × H) $mm^3$ | No. ports | Prototype | Fabrication materials | Antenna operating frequency (GHz) | Bandwidth (GHz) | Max. gain (dBi) | Efficiency (%) | Max. isolation ratio (dB) | ECC | DG (dB) | CCL (bits/s /Hz) |
|---|---|---|---|---|---|---|---|---|---|---|---|---|---|
| 77] | 2023 | 50 × 62 × 0.8 | 4 |  | • Copper<br>• FR4<br>($\varepsilon_r = 4.4$ and $\delta = 0.02$) | 4.4–4.9<br>5.4–6.1<br>7.0–7.4 | 0.5<br>0.7<br>0.4 | 3.1 | NA* | −55 | $<0.04$ | NA* | $\leq 0.4$ |
| [78] | 2023 | 50 × 50 × 12.5 | 4 | 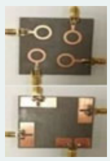 | • Copper<br>• Rogers 5880<br>($\varepsilon_r = 2.2$ and $\delta = 0.0009$) | 3.3–5.8 | 2.5 | 3.8 | NA* | −30 | $<0.05$ | 9.9 | $<0.4$ |
| [79] | 2023 | 42 × 42 × 1 | 4 |  | • Copper<br>• FR4<br>($\varepsilon_r = 4.4$ and $\delta = 0.02$) | 3.09–12 | 8.91 | 5.1 | 82 | −55 | $<0.02$ | 9.9 | NA* |
| [80] | 2023 | 80 × 80 × 1.6 | 4 | 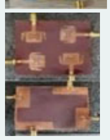 | • Copper<br>• FR4<br>($\varepsilon_r = 4.4$ and $\delta = 0.02$) | 2.4–18 | 15.6 | 5.9 | 82 | −66 | $<0.03$ | 9.9 | NA* |
| [81] | 2023 | 35 × 35 × 1.6 | 4 |  | • Copper<br>• FR4<br>($\varepsilon_r = 4.3$ and $\delta = 0.025$) | 3.1–10.6 | 7.5 | NA* | NA* | −49 | $<0.022$ | 9.89 | $<0.4$ |
| [82] | 2023 | 54 × 54 × 1.52 | 4 |  | • Copper<br>• TLY 5 lossy<br>($\varepsilon_r = 2.2$ and $\delta = 0.0009$) | 3.1–11.8 | 8.7 | 6.6 | NA* | −49 | $<0.001$ | 9.99 | $<0.4$ |
| [83] | 2023 | 70 × 70 × 1.6 | 4 | 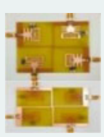 | • Copper<br>• FR4<br>($\varepsilon_r = 4.4$ and $\delta = 0.02$) | 2.25–2.9<br>3.4–3.9<br>4.7–6 | 0.65<br>0.5<br>1.3 | 1.74 | 85 | −50 | $<0.5$ | 9.9 | NA* |
| [84] | 2023 | 86 × 118 × 1.67 | 4 |  | • Copper<br>• Rogers 3035<br>($\varepsilon_r = 3.6$ and $\delta = 0.0015$) | 2–6.5<br>7.5–20 | 4.5<br>12.5 | 4.14 | NA* | −58 | $<0.0065$ | 9.5 | $<0.25$ |
| [85] | 2023 | 104 × 30 × 0.4 | 4 | 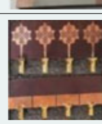 | • Copper<br>• Polyamide | 4.25–7.95 | 3.7 | 5.44 | 97.6 | −52 | $<0.05$ | 9.9 | NA* |
| [86] | 2023 | 40 × 40 × 1.6 | 4 | 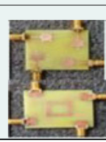 | • Copper<br>• FR4<br>($\varepsilon_r = 4.3$ and $\delta = 0.002$) | 3.2–12.44 | 9.24 | 4.9 | 89 | −46 | $<0.0016$ | 9.96 | $<0.4$ |

(*Continued*)

Moreover, in the manuscript [121], the authors presented a new geometry for an eight-port antenna with geometric dimensions (150 × 80 × 1.6 $mm^3$), as shown in Fig. 20. The authors focused on presenting an antenna composed of four elements, each containing two ports. Note that the antenna was designed with both simulation aspects using the HFSS software (version

https://doi.org/10.1017/S1759078724001004 Published online by Cambridge University Press

**Table 3.** (*Continued.*)

| Ref. | Year | Antenna dimensions (W × L × H) $mm^3$ | No. ports | Prototype | Fabrication materials | Antenna operating frequency (GHz) | Bandwidth (GHz) | Max. gain (dBi) | Efficiency (%) | Max. isolation ratio (dB) | ECC | DG (dB) | CCL (bits/s /Hz) |
|---|---|---|---|---|---|---|---|---|---|---|---|---|---|
| [87] | 2023 | 58.6 × 58.6 × 1.6 | 4 | 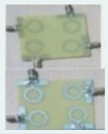 | • Copper<br>• FR4<br>($\varepsilon_r = 3.5$ and $\delta = 0.02$) | 3.3–3.7 | 0.4 | 4.7 | 87 | −28 | $<0.04$ | NA* | $<0.3$ |
| [88] | 2023 | 40 × 40 × 1.6 | 4 | 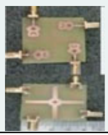 | • Copper<br>• FR4<br>($\varepsilon_r = 4.3$ and $\delta = 0.002$) | 3.1–10.6 | 7.5 | 6 | 91 | −52 | $<0.0011$ | 9.9 | $<0.28$ |

**Table 4.** A summary of the most recent research on quad-port antennas designed for mmWave frequency bands

| Ref. | Year | Antenna dimensions (W × L × H) $mm^3$ | No. ports | Prototype | Fabrication materials | Antenna operating frequency (GHz) | Bandwidth (GHz) | Max. gain (dBi) | Efficiency (%) | Max. isolation ratio (dB) | ECC | DG (dB) | CCL bits/s/Hz |
|---|---|---|---|---|---|---|---|---|---|---|---|---|---|
| [89] | 2023 | 40 × 40 × 0.8 | 4 | 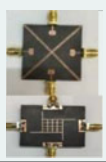 | • Copper<br>• Rogers<br>5880 (($\varepsilon_r = 2.2$ and $\delta = 0.0009$) | 22.4–30 | 7.6 | 6.87 | 97 | −39.90 | $<0.005$ | 9.9 | $<0.4$ |
| [90] | 2023 | 22 × 22 × 0.79 | 4 | 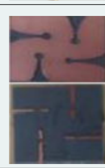 | • Copper<br>• Rogers<br>5880 ($\varepsilon_r = 2.2$ and $\delta = 0.0009$) | 26.31–30.95<br>38.35–41.04 | 4.64<br>2.69 | 5.65<br>5.53 | NA* | −48 | $<0.001$ | 9.99 | $<0.4$ |
| [91] | 2023 | 40 × 40 × 18 × 0.508 | 4 |  | • Copper<br>• Rogers<br>5880 ($\varepsilon_r = 2.2$ and $\delta = 0.0009$) | 24.5–25.5<br>28.5–32 | 1<br>3.5 | 7.9<br>7.5 | 9295 | −69 | $<0.0001$ | 9.99 | $<0.4$ |
| [92] | 2023 | 48 × 12 × 0.254 | 4 |  | • Copper<br>• Rogers<br>5880 ($\varepsilon_r = 2.2$ and $\delta = 0.0009$) | 23–33<br>37.75–41 | 10<br>3.25 | 5.7 | 95 | −53 | $<0.00015$ | 9.99 | NA* |
| [93] | 2023 | 25 × 25 × 0.787 | 4 |  | • Copper<br>• Rogers<br>5880 $\varepsilon_r = 2.2$ and $\delta = 0.0009$) | 25.28–28.02 | 2.74 | 8.72 | NA* | −46 | $<0.0015$ | 9.99 | NA* |
| [94] | 2023 | 33 × 33 × 0.203 | 4 | 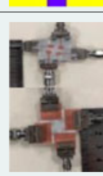 | • Copper<br>• Rogers<br>4003C ($\varepsilon_r = 3.55$ and $\delta = 0.0027$) | 25–50 | 25 | NA* | 80–92 | −51 | $<0.005$ | 9.99 | $<0.3$ |
| [95] | 2023 | 31.7 × 31.7 × 1.6 | 4 |  | • Copper<br>• FR4<br>($\varepsilon_r = 4.4$ and $\delta = 0.02$) | 3–17<br>25.3–35.1<br>35.5–49.4 | 14<br>9.8<br>13.9 | 3.03<br>5.87<br>5.92 | 56.7<br>58.8<br>52.5 | −55 | $<0.21$<br>$<0.034$<br>$<0.04$ | 9.99 | $<0.6$ |

(*Continued*)

https://doi.org/10.1017/S1759078724001004 Published online by Cambridge University Press

**Table 4.** (*Continued.*)

| Ref. | Year | Antenna dimensions (W × L × H) $mm^3$ | No. ports | Prototype | Fabrication materials | Antenna operating frequency (GHz) | Bandwidth (GHz) | Max. gain (dBi) | Efficiency (%) | Max. isolation ratio (dB) | ECC | DG (dB) | CCL bits/s/Hz |
|---|---|---|---|---|---|---|---|---|---|---|---|---|---|
| [96] | 2023 | 26 × 26 × 0.25 | 4 |  | • Copper<br>• Rogers<br>3003 ($\varepsilon_r = 3$ and $\delta = 0.001$) | 27.7–28.3<br>37.7–38.3 | 0.6<br>0.6 | 7.4<br>8.1 | 88<br>88.8 | −59 | $<$0.0085 | 9.99 | $<$0.3 |
| [97] | 2023 | 20 × 20 × 0.254 | 4 | 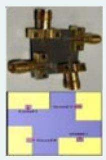 | • Copper<br>• Rogers<br>5880 ($\varepsilon_r = 2.2$ and $\delta = 0.009$) | 25–28 | 3 | 6.2 | $>$88 | −22 | $<$0.012 | 9.88 | $<$0.5 |
| [98] | 2023 | 36 × 36 × 0.8<br>45 × 45 × 0.8 | 4<br>4 |  | • Copper<br>• Rogers<br>5880 ($\varepsilon_r = 2.2$ and $\delta = 0.0009$) | 27.2–28.85 | 1.65 | 7.2<br>8.6 | 86 | −46 | $<$0.002<br>$<$0.002 | 9.99 | NA* |
| [99] | 2023 | 12 × 45.2 × 0.254 | 4 |  | • Copper<br>• Rogers<br>5880 ($\varepsilon_r = 2.2$ and $\delta = 0.0009$) | 24.86–41.48 | 16.62 | 12.02 | $>$80 | −33 | $<$0.0014 | 9.99 | $<$0.29 |
| [100] | 2023 | 31.5 × 45 × 0.254 | 4 |  | • Copper<br>• Rogers<br>5880 ($\varepsilon_r = 2.2$ and $\delta = 0.0009$) | 23.5–31.72 | 8.22 | 6.5 | NA* | −50 | $<$0.18 | 10 | $<$0.25 |
| [101] | 2022 | 14 × 14 × 0.8 | 4 | 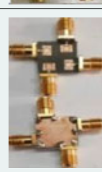 | • Copper<br>• Rogers<br>5880 ($\varepsilon_r = 2.2$ and $\delta = 0.0009$) | 26.6–2937.3–39.3 | 2.4<br>2 | 8.46.02 | 91.66<br>88.57 | −42 | $<$0.005 | 9.99 | $<$0.35 |
| [102] | 2023 | 32 × 32 × 0.7874 | 4 | 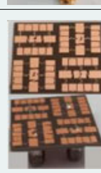 | • Copper<br>• Rogers<br>5880 $= 2.2$ and $\delta = 0.0009$) | 24.6–30.6 | 6 | 12.4 | 92 | −59 | $<$0.0002 | 9.99 | NA* |
| [103] | 2022 | 34 × 34 × 0.835 | 4 | 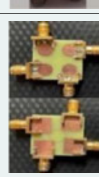 | • Copper<br>• Rogers<br>5880($\varepsilon_r = 2.2$ and $\delta = 0.0009$) | 24.8–44.45 | 19.65 | 8.6 | 85 | −35 | $<$0.008 | 9.96 | NA* |
| [104] | 2022 | 24 × 24 × 0.254 | 4 |  | • Copper<br>• Rogers<br>5880 ($\varepsilon_r = 2.3$ and $\delta = 0.0009$) | 22–40 | 18 | 7.1 | 92 | −55 | $<$0.05 | NA* | NA* |
| [105] | 2024 | 30 × 30 × 0.254 | 4 | 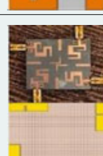 | • Copper<br>• Rogers<br>5880 ($\varepsilon_r = 2.3$ and $\delta = 0.0009$) | 5.2–5.7<br>11.8–17.3<br>23.4–37.3 | 0.5<br>5.5<br>13.9 | 3.05<br>5.27<br>6.67 | 93–98 | −55 | $<$0.004<br>$<$ 0.002<br>$<$ 0.002 | $>$9.9<br>$>$ 9.9<br>$>$ 9.9 | $<$0.4 |

(*Continued*)

https://doi.org/10.1017/S1759078724001004 Published online by Cambridge University Press

**Table 4.** (*Continued.*)

| Ref. | Year | Antenna dimensions (W × L × H) $mm^3$ | No. ports | Prototype | Fabrication materials | Antenna operating frequency (GHz) | Bandwidth (GHz) | Max. gain (dBi) | Efficiency (%) | Max. isolation ratio (dB) | ECC | DG (dB) | CCL bits/s/Hz |
|---|---|---|---|---|---|---|---|---|---|---|---|---|---|
| [106] | 2023 | 2.4.7 × 24.7 × 0.8 | 4 | 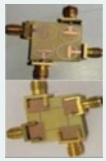 | • Copper<br>• Rogers<br>5880 ($\varepsilon_r = 2.2$ and $\delta = 0.0009$) | 27.12–31.34<br>37.21–38.81 | 4.22<br>1.6 | 5.75<br>5.62 | 85 | −50 | $<0.04$ | $>9.5$ | NA* |
| [107] | 2023 | 25.95 × 25.95 × 0.238 | 4 |  | • Copper<br>• Rogers<br>5880 $= 2.2$ and $\delta = 0.0009$) | 37–39 | 2 | 8.2–10 | 82 | −31 | $<0.005$ | 9.99 | $<0.4$ |
| [108] | 2023 | 27 × 27 × 1.52 | 4 |  | • Copper<br>• Rogers<br>6002 ($\varepsilon_r = 2.2$ and $\delta = 0.0012$) | 26.5–43.7 | 17.2 | 8.4 | NA* | −42 | $<0.001$ | 9.99 | $<0.4$ |
| [109] | 2023 | 52 × 52 × 1.6 | 4 |  | • Copper<br>• FR4<br>($\varepsilon_r = 4.4$ and $\delta = 0.02$) | 1.25–3<br>3.2–6<br>6.2–9<br>9.1–43 | 1.75<br>2.8<br>2.8<br>33.9 | 4 | 86 | −55 | $<0.01$ | NA* | NA* |
| [110] | 2023 | 30 × 30 × 0.203 | 4 |  | • Copper<br>• Rogers<br>4003 ($\varepsilon_r = 3.55$ and $\delta = 0.0027$) | 58–63 | 5 | 9.2 | NA* | −50 | $<0.002$ | $>9.99$ | NA* |
| [111] | 2024 | 45 × 45 × 0.25 | 4 |  | • Copper<br>• Rogers<br>3003 ($\varepsilon_r = 3$) | 24.7–31.6 | 6.9 | 10.3 | 88 | −55 | $<0.0006$ | 9.99 | NA* |
| [112] | 2022 | 30 × 30 × 1.575 | 4 | 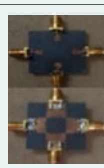 | • Copper<br>• Rogers<br>5880 $= 2.2$ and $\delta = 0.0009$) | 26.4–29.75 | 3.35 | 7.1 | NA* | −45 | $<0.0005$ | 9.999 | 0.15 |
| [113] | 2021 | 20 × 24 × 0.508 | 4 | 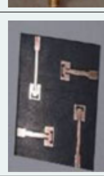 | • Copper<br>• Rogers<br>5880 ($\varepsilon_r = 2.2$ and $\delta = 0.0009$) | 27.6–28.6<br>37.4–38.6 | 1<br>1.2 | 7.1<br>7.9 | $>85$ | −53 | $<0.001$ | NA* | NA* |
| [114] | 2021 | 30 × 30 × 0.787 | 4 | 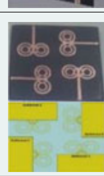 | • Copper<br>• Rogers<br>5880 ($\varepsilon_r = 2.2$ and $\delta = 0.0009$) | 26.5–28.5 | 2 | 6.1 | 92 | −45 | $<0.16$ | NA* | NA* |
| [115] | 2021 | 47.4 × 32.5 × 0.51 | 4 | 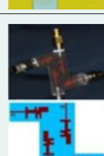 | • Copper<br>• Rogers<br>5880 ($\varepsilon_r = 2.2$ and $\delta = 0.0009$) | 36.86–40 | 3.14 | 6.5 | $>80$ | −45 | $<0.001$ | 9.99 | $<0.6$ |

(*Continued*)

**Table 4.** (*Continued.*)

| Ref. | Year | Antenna dimensions (W × L × H) $mm^3$ | No. ports | Prototype | Fabrication materials | Antenna operating frequency (GHz) | Bandwidth (GHz) | Max. gain (dBi) | Efficiency (%) | Max. isolation ratio (dB) | ECC | DG (dB) | CCL bits/s/Hz |
|---|---|---|---|---|---|---|---|---|---|---|---|---|---|
| [116] | 2022 | 75 × 150 × 0.25 | 4 |  | • Copper<br>• Rogers<br>3003<br>($\varepsilon_r = 3$<br>and<br>$\delta = 0.0021$) | 28 and<br>38 GHz | 0.6<br>1.17 | 4.7<br>3.75 | 88<br>90 | −65 | $<0.0006$ | $>9.997$ | NA* |
| [117] | 2021 | 79.4 × 9.65 × 0.25 | 4 |  | • Copper<br>• Rogers<br>3003<br>($\varepsilon_r = 3$<br>and<br>$\delta = 0.0021$) | 28 and<br>38 GHz | 3.42<br>1.45 | 9 | NA* | −60 | $<0.0008$ | $>9.996$ | NA* |
| [118] | 2022 | 28 × 28 × 0.79 | 4 |  | • Copper<br>• Rogers<br>5870<br>($\varepsilon_r = 2.33$<br>and<br>$\delta = 0.0012$) | 26.5–31.5<br>36–41.7 | 5<br>5.7 | 9.5<br>11.5 | NA* | −50 | $<0.001$ | 9.99 | $<0.4$ |
| [119] | 2022 | 20 × 20 × 0.8 | 4 |  | • Copper<br>• Rogers<br>5880<br>$= 2.2$ and<br>$\delta = 0.0009$) | 26.867–28.975 | 2.1 | 9.24 | 78.6 | −45 | $<0.0013$ | 9.4 | NA* |

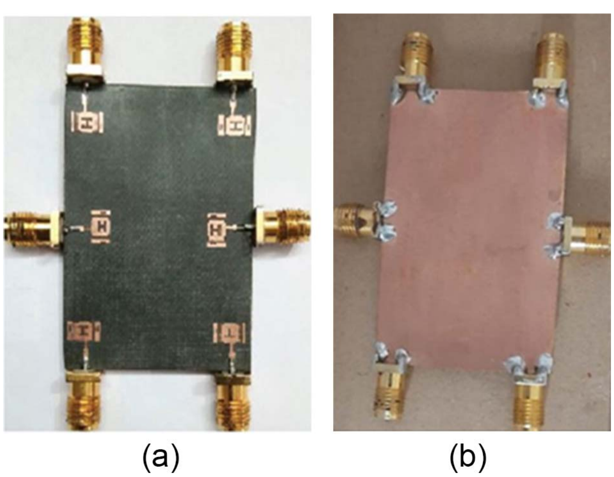

**Figure 17.** The structural manufacturing design of the proposed antenna for (a) the front face and (b) the back face [120].

2020), as shown in Fig. 20, and actual fabrication using practical laboratories, as shown in Figs. 21(a) and (b). The materials for manufacturing the antenna are copper for the patch and ground layers and FR4 (permittivity of 4.4 and tangent loss of 0.02) for the substrate layer. This antenna operates at sub-6 GHz frequencies ranging from 3.4 to 3.6 GHz, as shown in Fig. 22(a). The antenna achieved the lowest isolation value between the two ports (first and second) of −14 dB and the highest value between the two ports (first and fourth) of −43 dB, as shown in Fig. 22(b). It also achieved good performance values for the ECC parameter $<0.065$, with the highest gain reaching 6.24 dB. The efficiency for the simulation side ranges between 75% and 85%, and the practical side ranges between 60% and 75%, as shown in Fig. 23.

Furthermore, several recent studies have introduced MIMO antennas with eight or more ports. Summaries of designs operating at sub-27 GHz and mmWave frequencies are provided in Tables 5 and 6, respectively. In these studies, increasing the number of ports while reducing the antenna size has increased mutual coupling between MIMO antenna elements and deteriorated the results in some works.

## Importance of equivalent circuits for antennas

In recent years, an equivalent circuit representation of antennas has gained popularity. A wide variety of studies have utilized the model to either build a custom antenna or analyze and isolate the lost parts of the antenna [149]. On the other hand, multi-antennas, like these in the MIMO system, have received less attention. Adding more antennas to the system with MIMO technology may significantly increase the data capacity and performance of the system. To improve communication capacity in MIMO systems, researchers implemented the space decoupling approach, also known as the network decoupling technique. As a result, a robust equivalent circuit simulation is crucial for designing and evaluating separation techniques [150]. Additionally, equivalent circuit models, also known as network models, have attracted attention for their ability to facilitate the study of circuit effects such as amplifier noise, matching, and reconfigurability.

These models also allow the simulation of combined antenna arrays and multiuser MIMO systems [151]. These particular types of models are appealing from a computational standpoint because both transmit and receive arrays may be expressed as comparable circuits. This means that a small number of full-wave computations

https://doi.org/10.1017/S1759078724001004 Published online by Cambridge University Press

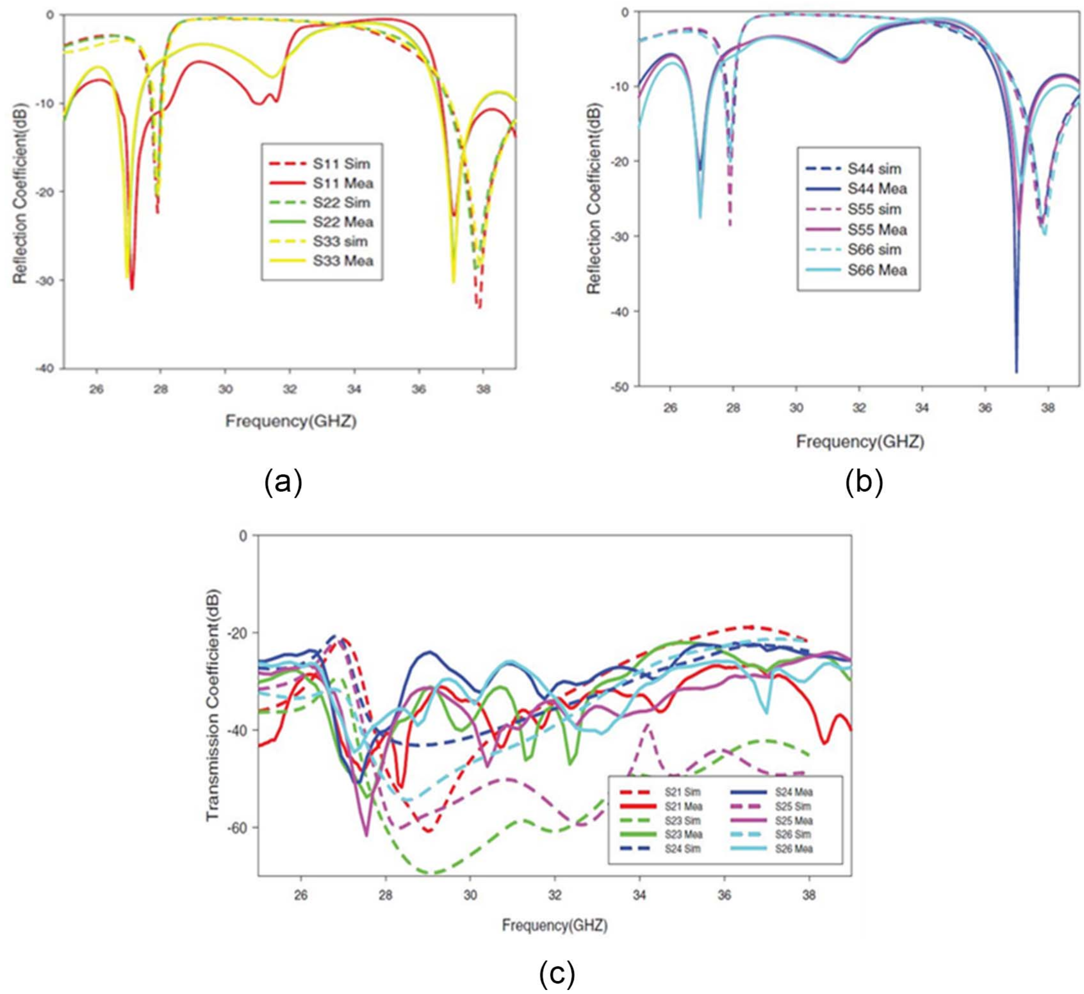


**Figure 18.** Antenna performance measurement curves for (a) and (b) reflection coefficient and (c) transmission coefficient [120].

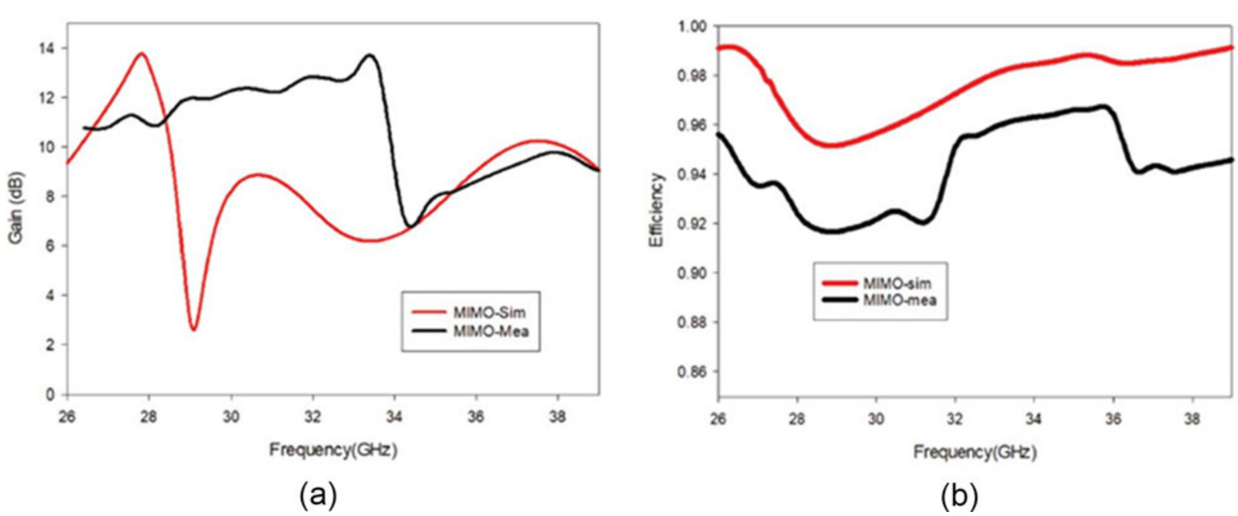


**Figure 19.** The complementary results achieved by the antenna are (a) gain curves for both sides of CST simulation and actual measurements, and (b) total efficiency curves for simulation and manufacturing [120].

or measurements are needed, and then circuits with different levels of complexity can be examined through effective circuit-level modeling. As officially shown in reference [152], a similar impedance matrix (apart from a transpose) can be used for both modes of operation. This implies that network analysis can be used to model an antenna array in both transmission and reception modes. An

https://doi.org/10.1017/S1759078724001004 Published online by Cambridge University Press

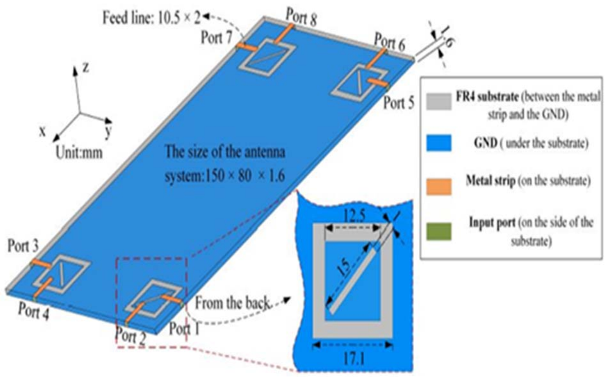


**Figure 20.** A geometric design of the proposed octa-port MIMO antenna using the HFSS simulation program [121].

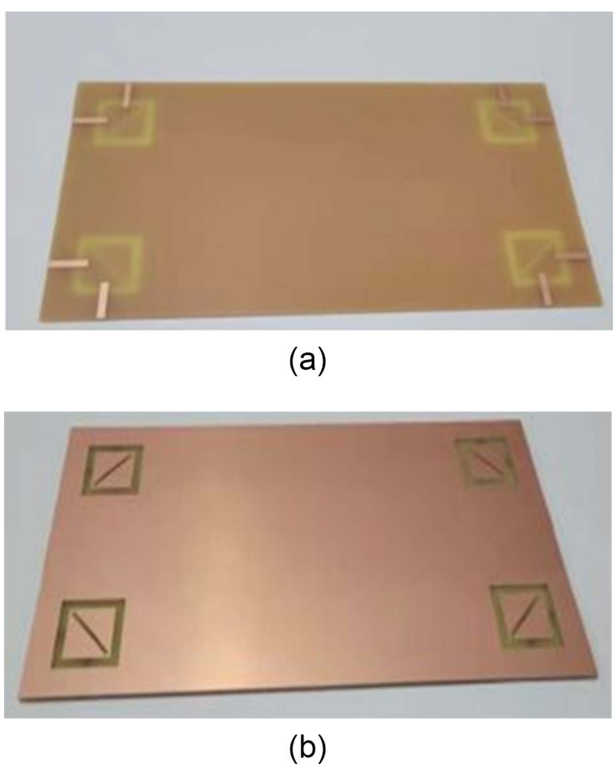


**Figure 21.** The fabrication geometry of the proposed MIMO antenna for (a) the front view and (b) the back view [121].

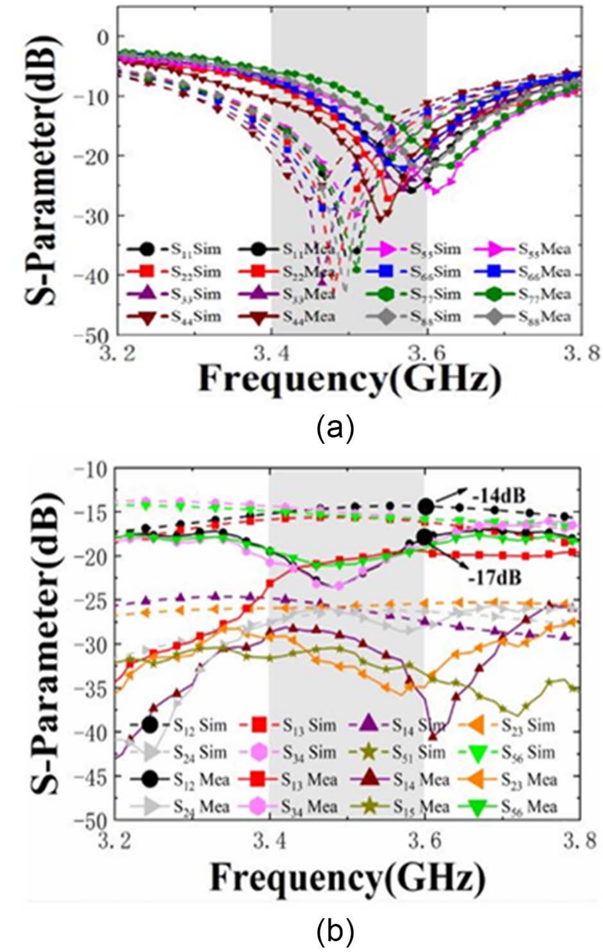


**Figure 22.** (a) The reflection coefficients for the simulation and fabrication aspects, and (b) the mutual coupling between all ports [121].

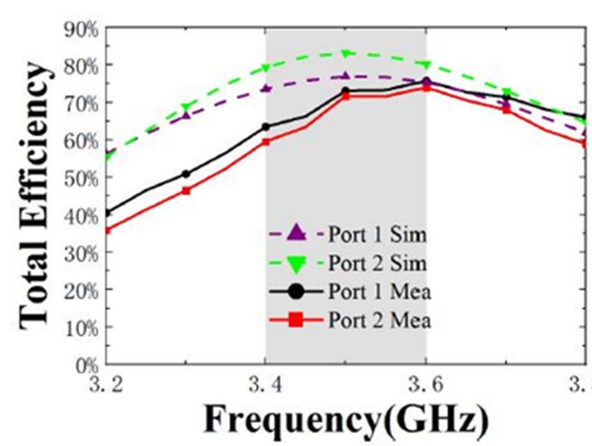


**Figure 23.** Overall antenna efficiency for all simulations and fabrication measurements [121].

equivalent model was used to study how mutual coupling affects adaptive arrays. It created a beamformer to improve the signal-to-interference-to-noise ratio (SINR) and showed its relationship with loaded voltages and open circuits in the receiving array [153].

## Challenges, developments, and future directions discussion

Massive MIMO (M-MIMO) antennas outperform traditional multi-antenna systems. MIMO and 5G technologies might revolutionize wireless networking. Nevertheless, various issues persist that impede the actual application of M-MIMO. For each type of application, hardware components confront several challenges, including material selection, size, cost, and characteristic properties (bandwidth, efficiency, gain, mutual coupling, and so on) [154].

Many design issues will arise due to the wide variety of devices, and the 5G frequency range will exacerbate them. The spectrum must be adaptable to accommodate devices that operate on different spectral bands. There has been an increasing focus on the sub-6 GHz band for 5G communication to address these challenges,

https://doi.org/10.1017/S1759078724001004 Published online by Cambridge University Press

**Table 5.** A detailed comparison of the latest articles proposing eight-port antennas operates at frequencies sub-27 GHz

| Ref. | Year | Antenna dimensions ($W \times L \times H$) $mm^3$ | No. ports | Prototype | Fabrication materials | Antenna operating frequency (GHz) | Bandwidth (GHz) | Max. gain (dBi) | Efficiency (%) | Max. isolation ratio (dB) | ECC | DG (dB) | CCL (bits/s/Hz) |
|---|---|---|---|---|---|---|---|---|---|---|---|---|---|
| [122] | 2023 | 150 × 75 × 1.6 | 8 |  | • Copper<br>• FR4<br>($\varepsilon_r = 4.3$ and $\delta = 0.025$) | 3.3–4. 1 | 0.8 | 4.1 | 85 | −50 | <0.001 | NA* | <0.44 |
| [123] | 2023 | 60 × 60 × 1.6 | 8 | 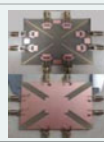 | • Copper<br>• FR4<br>($\varepsilon_r = 4.3$ and $\delta = 0.025$) | 14–18 | 4 | 6.32 | 80 | −50 | <0.008 | 9.96 | 0.5 |
| [124] | 2023 | 150 × 75 × 0.8 | 8 | 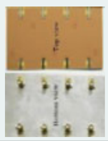 | • Copper<br>• FR4<br>$= 4.4$ and $\delta = 0.02$) | 3.6–4.7 | 1.1 | 1.5 | 87 | −55 | <0.08 | NA* | NA* |
| [125] | 2023 | 75 × 150 × 1.6 | 8 |  | • Copper<br>• Rogers 5880<br>($\varepsilon_r = 2.2$ and $\delta = 0.0009$) | 3.5–3.7 | 0.2 | 4.5 | 80 | −50 | <0.004 | NA* | <0.5 |
| [126] | 2024 | 150 × 75 × 1.6 | 8 | 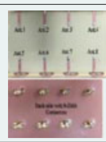 | • Copper<br>• FR4<br>($\varepsilon_r = 4.3$ and $\delta = 0.025$) | 3.4–3.6<br>4.8–5.8 | 0.2<br>1 | 5.8 | 71 | −70 | <0.04 | NA* | <0.385 |
| [127] | 2024 | 48 × 48 × 1.6 | 8 |  | • Copper<br>• FR4<br>($\varepsilon_r = 4.4$ and $\delta = 0.02$) | 3.557 to 3.767 | 0.21 | NA* | NA* | −80 | <0.0001 | 9.99 | NA* |
| [128] | 2024 | 150 × 80 × 1.6 | 8 | 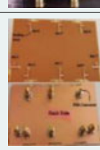 | • Copper<br>• FR4<br>($\varepsilon_r = 4.4$ and $\delta = 0.02$) | 3.4–3.6<br>4.6–4.87 | 0.2<br>0.27 | 3.2 | 71 | −31 | <0.05 | NA* | NA* |
| [129] | 2023 | 72 × 72 × 1.6 | 8 | 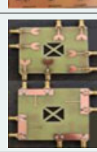 | • Copper<br>• FR4<br>( $= 4.3$ and $\delta = 0.025$) | 3.3–6 | 2.7 | 2.5 | 95 | −52 | <0.005 | 9.99 | <0.05 |
| [130] | 2023 | 105 × 60 × 1.6 | 8 |  | • Copper<br>• FR4<br>($\varepsilon_r = 4.4$ and $\delta = 0.02$) | 3.2–3.55 | 0.35 | NA* | 70 | −66 | <0.03 | NA* | NA* |
| [131] | 2023 | 150 × 75 × 0.8 | 8 |  | • Copper<br>• FR4<br>($\varepsilon_r = 4.3$ and $\delta = 0.025$) | 3.4–3.65 | 0.25 | 4.8 | 76 | −35 | <0.01 | 9.99 | <0.435 |

(*Continued*)

offering an effective solution. Base station approaches in 5G sub-6 GHz employ single and multiband designs over several kinds of bands of frequencies, which provide specific challenges. Utilizing various array geometries, such as patch sub-arrays, multimode-slotted designs, and other configurations [155], can lead to high gain and effective performance. Because the current concerns

https://doi.org/10.1017/S1759078724001004 Published online by Cambridge University Press

**Table 5.** (*Continued*.)

| Ref. | Year | Antenna dimensions ($W \times L \times H$) $mm^3$ | No. ports | Prototype | Fabrication materials | Antenna operating frequency (GHz) | Bandwidth (GHz) | Max. gain (dBi) | Efficiency (%) | Max. isolation ratio (dB) | ECC | DG (dB) | CCL (bits/s/Hz) |
|---|---|---|---|---|---|---|---|---|---|---|---|---|---|
| [132] | 2023 | 140 × 70 × 0.8 | 8 |  | • Copper<br>• FR4<br>($\varepsilon_r = 4.4$ and $\delta = 0.02$) | 3.28–5.05 | 1.77 | NA* | 82 | −36 | $<0.01$ | 9.9 | $<0.352$ |
| [133] | 2023 | 70 × 70 × 1.6 | 8 |  | • Copper<br>• FR4<br>($\varepsilon_r = 4.3$ and $\delta = 0.025$) | 3.15–6 | 2.85 | 7.6 | NA* | −50 | $<0.004$ | 9 | NA* |
| [134] | 2023 | 66 × 66 × 1.6 | 8 |  | • Copper<br>• FR4<br>($\varepsilon_r = 4.3$ and $\delta = 0.025$) | 3.7–4.5<br>5.1–5.9<br>7.9–14.3 | 0.8<br>0.8<br>6.4 | 6.8 | 90 | −60 | $<0.020$ | 9.9 | $<0.8$ |
| [135] | 2023 | 150 × 75 × 3.5 | 8 | 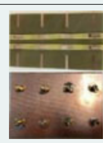 | • Copper<br>• FR4<br>($\varepsilon_r = 4.4$ and $\delta = 0.02$) | 3.1–3.7<br>4.47–4.91<br>5.5–6.0 | 0.6<br>0.44<br>0.5 | 5.8 | 78 | −60 | $<0.025$ | 9.84 | $<0.411$ |
| [136] | 2023 | 76 × 76 × 40 | 8 |  | • Copper<br>• FR4<br>($\varepsilon_r = 4.3$ and $\delta = 0.025$) | 1.7–1.9<br>2.3–2.6<br>5.1–5.5<br>5.7–6.3 | 0.2<br>0.3<br>0.4<br>0.6 | 4.2 | 80 | −70 | $\leq 0.1$ | 9.99 | $\leq 0.25$ |
| [137] | 2023 | 150 × 70 × 7 | 8 | 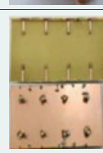 | • Copper<br>• FR4<br>($\varepsilon_r = 4.4$ and $\delta = 0.02$) | 3.0–5.3 | 2.3 | 5.3 | 75 | −39 | $<0.08$ | NA* | $<0.46$ |
| [138] | 2023 | 150 × 75 × 7 | 8 | 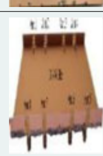 | • Copper<br>• FR4<br>($\varepsilon_r = 4.4$ and $\delta = 0.02$) | 3.3–5 | 1.7 | 3 | 80 | −42 | $<0.12$ | NA* | $<0.38$ |
| [139] | 2023 | 150 × 70 × 7 | 8 |  | • Copper<br>• FR4<br>($\varepsilon_r = 4.4$ and $\delta = 0.02$) | 2.01–5.23 | 3.22 | 3 | 75 | −25 | $<0.02$ | 9.9 | NA* |
| [140] | 2023 | 143.2 × 73.2 × 1.6 | 8 | 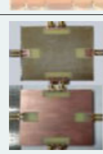 | • Copper<br>• FR4<br>($\varepsilon_r = 4.3$ and $\delta = 0.025$) | 3.29–3.66 | 0.37 | NA* | 75 | −40 | $<0.02$ | NA* | $<0.0125$ |
| [141] | 2023 | 70 × 70 × 1.6 | 8 | 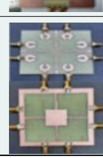 | • Copper<br>• FR4<br>($\varepsilon_r = 4.4$ and $\delta = 0.02$) | 3.75–5.75 | 2 | 7.8 | 88 | −47 | $<0.05$ | 9.9 | $<0.4$ |

are about antenna placement, number requirements, and mutual interference prevention – especially in light of the new desire for a 5G network – frequencies do not provide a wide range of issues [156].

An antenna has a fixed number of components arranged in symmetrical and asymmetrical array designs. As an illustration of base station approaches, symmetric and asymmetric planar structures are rectangular arrays, such as the (4 × 4) and (4 × 1) designs of elements. Regarding the radiation patterns' effectiveness, gain, and directivity, they examined the effects of one of the elements in addition to the arrays through antenna configuration. In the design of smartphones, antennas are positioned at the edges in a symmetrical or nonsymmetrical manner for two sides or one side, as in the (8 × 8) model of components, where each of the four is located at

https://doi.org/10.1017/S1759078724001004 Published online by Cambridge University Press

**Table 6.** A comparison of recent research on eight-port or more antennas relying on mmWave bands

| Ref. | Year | Antenna dimensions ($W \times L \times H$) $mm^3$ | No. ports | Prototype | Fabrication materials | Antenna operating frequency (GHz) | Bandwidth (GHz) | Max. gain (dBi) | Efficiency (%) | Max. isolation ratio (dB) | ECC | DG(dB) | CCL (bits/s/Hz) |
|---|---|---|---|---|---|---|---|---|---|---|---|---|---|
| [142] | 2023 | 18 × 45.6 × 0.254 | 8 |  | • Copper<br>• Rogers<br>5880 ($\varepsilon_r = 2.2$ and $\delta = 0.0009$) | 22–40 | 18 | 5 | 75 | −48 | ≤0.005 | 9.98 | NA* |
| [143] | 2023 | 81.6 × 62.4 × 13.822 | 8 | 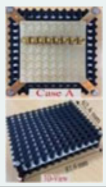 | • Copper<br>• Rogers<br>4450 F($\varepsilon_r$= 2.65) & 4350B ($\varepsilon_r$= 2.1) | 24.9–29.9 | 5 | NA* | 62.5–74 | −35 | NA* | NA* | NA* |
| [144] | 2023 | 27.2 × 27.2 × 1.6 | 8 | 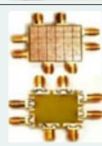 | • Copper<br>• FR4 ($\varepsilon_r = 4.4$ and $\delta = 0.02$) | 21–33 | 12 | 17 | NA* | −53 | <0.36 | 9.96 | NA* |
| [145] | 2022 | 43.7 × 118 × 0.8 | 8 |  | • Copper<br>• Roger<br>4350B ($\varepsilon_r = 3.48$ and $\delta = 0.0037$) | 28.5–29.5 | 1 | 11.7 | 90 | −42 | <0.3 | > 8.7 | NA* |
| [146] | 2019 | 200 × 100 × 21.2 × **0.8** | |  | • Copper<br>• FR4<br>($\varepsilon_r = 4.4$ and $\delta = 0.02$) | 20–40 | 20 | NA* | NA* | −65 | <0.0002 | 9.96 | NA* |
| [147] | 2022 | 39 × 44.2 × 0.254 | 8 | 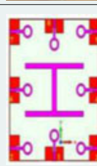 | • Copper<br>• Rogers<br>5880 ($\varepsilon_r = 2.2$ and $\delta = 0.0009$) | 24–34 | 10 | 5.9 | 99 | −55 | <0.12 | 9.92 | NA* |
| [148] | 2024 | 30 × 200 × 0.787 | 16 |  | • Copper<br>• Rogers<br>5880 ($\varepsilon_r = 2.2$ and $\delta = 0.0009$) | 25.5–29 | 3.5 | 19.9 | 99 | −65 | <0.008 | 9.94 | <0.4 |

an edge. These results are excellent with set element spacing and complete isolation [157].

It can be challenging to assess how closely spaced MIMO antenna components negatively affect mutual coupling [158]. However, the small size and decoupling techniques have significantly resolved the issue by improving isolation between the antennas, thereby positively impacting the characteristics. The antennas' small size and compact design could have contributed to their excellent spectrum efficiency and minimal mutual coupling. It should be mentioned that M-MIMO base stations are now supported through both 2D and 3D positioning of antenna components. Nevertheless, applying 2D or 3D antenna arrays can significantly increase energy efficiency and improve coupling effects. Utilizing decoupling methods to expand the separation of array elements is a feasible approach that enhances spectral efficiency. For improved results, a small 3D array M-MIMO antenna can be employed using or without decoupling techniques like hexagonal, triangular, and cylindrical models. One of the primary characteristics of 5G MIMO antennas is decoupling techniques, which are necessary due to the size of smartphones and the design requirements for the massive methods [159, 160].

During the comprehensive review of many studies and recent works presented in this article, we concluded many points that will serve researchers in the future when they provide an ideal antenna, the most important of which are:

1. It was concluded that choosing the ideal materials involved in manufacturing the antenna plays an important role in improving the results of the antenna.

https://doi.org/10.1017/S1759078724001004 Published online by Cambridge University Press

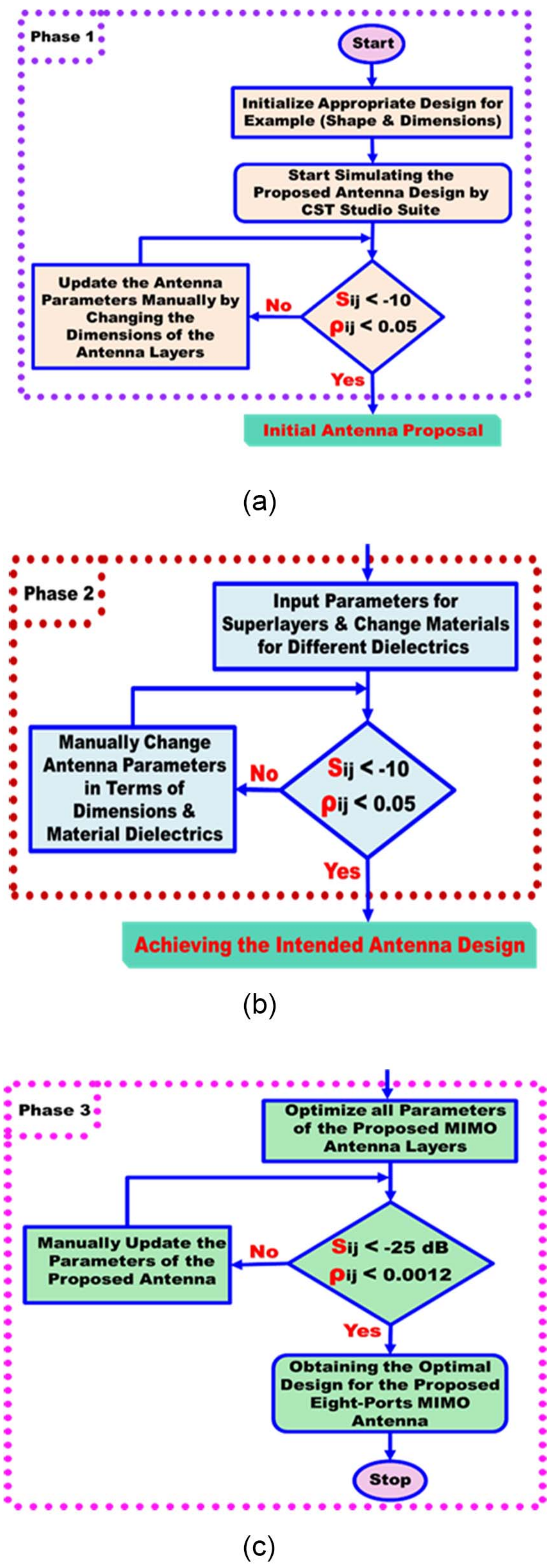


**Figure 24.** The proposed antenna design stages are (a) the first stage, (b) the second stage, and (c) the third stage.

2. It has been discovered that material properties such as dielectric constant and loss tangent also play an important role in achieving excellent results if chosen appropriately.


**Figure 25.** The primary challenges for designers in creating multiband MIMO antennas.

3. It has been noted that the thickness of the antenna layers has a major role in improving or deteriorating the antenna results.
4. It was also concluded that increasing the antenna ports in the MIMO configuration increases the mutual coupling between the antenna elements, and this will cause an increase in noise and interference between the electromagnetic signals fed to each port. Thus, the antenna's performance will degrade.
5. It was also discovered that the ideal MIMO antenna design consists of three stages, as shown in the flowchart in Figs. 24(a), (b) and (c).

Furthermore, the small size and ease of combining with other components are inherent advantages of planar antenna architectures, such as microstrip antennas. Generally, these antennas have a lower bandwidth and gain than 3D antennas. Likewise, they may be more susceptible to interference and coupling between MIMO ports. In contrast, the major challenges for antenna designers in creating an ideal multiband antenna are summarized in Fig. 25.

## Conclusions

An extensive study of design techniques, advancements, fabrication materials, difficulties, and MIMO antenna applications was provided in this article. The design of the antennas in this study was divided into two parts: the first part included broadband antennas, and the second part included mmWave antennas. In the first part, we presented a comprehensive study on the three most important types of MIMO antennas (two-, four-, and eight-port) that operate at frequencies between 1 and 27 GHz. In the second part, we discussed the designs of MIMO antennas based on the mmWave bands between 30 and 100 GHz for the three most in-demand types in the market (two-, quad-, and eight-port). In both parts, we compared the latest works presented by researchers in previous studies, and we focused in this comparison on the parameters that determine the ease of understanding the designs by the reader. These parameters are the geometric structure of the antenna, the number of ports, fabrication materials, the dimensions of the antenna (width × length × thickness), antenna operating frequencies, gain, port isolation techniques, overall efficiency, ECC, DG, and CCL.

https://doi.org/10.1017/S1759078724001004 Published online by Cambridge University Press

Therefore, we have drawn several conclusions that will serve future researchers when manufacturing ideal antennas. The most important of which is that fabrication materials play a major role in improving the performance of antennas. It was also noted that the mutual coupling between the ports in the MIMO configuration is greatly improved thanks to the use of many modern technologies simplified in this article. In addition, we concluded that antennas that operate at mmWave frequencies have small dimensions and suffer from isolation problems between the antenna elements in the MIMO formation. Unlike the antennas that operate at frequencies below 6 GHz, which have larger dimensions and do not suffer from isolation problems between the ports, this gives the best results, so it has become used in various modern wireless application systems. Furthermore, we concluded that all the work and comparisons presented will help all researchers provide high-performance MIMO antenna designs to meet the rapid development requirements in modern wireless communications and applications for the current 5G or future 6G systems. In the future, a MM technique with particular properties (isolating materials) will be used to address hardware challenges, component characteristics, modification, and enhancement. This will effectively lead to improvements in size, efficiency, gain, bandwidth, and several other aspects.

**Author contributions.** All authors contributed equally to data analysis, generating results, writing the article, and replying to reviews.

**Competing interests.** The authors report no conflict of interest (none declared).

## References


1. **Rani T, Chandra Das S, Hossen MS, Paul LC and Roy TK** (2022) Development of a broadband antenna for 5G sub-6 GHz cellular and IoT smart automation applications. In *2022 12th International Conference on Electrical and Computer Engineering (ICECE)*, 465–468.
2. **Muttair KS, Ghazi Zahid AZ, Shareef OA, HameedChyad Alfilh RH, Qasim Kamil AM and Mosleh MF** (2022) Design and analysis of wide and multi-bands multi-input multi-output antenna for 5G communications. *Indonesian Journal of Electrical Engineering and Computer Sciences* **26**(2), 903–914.
3. **Tao J and Feng Q** (2016) Compact ultrawideband MIMO antenna with half-slot structure. *IEEE Antennas and Wireless Propagation Letters* **16**, 792–795.
4. **Paul LC, Ahmed Ankan SS, Rani T, Rahman Jim MT, Karaaslan M, Shezan SA and Wang L** (2023) Design and characterization of a compact four-element microstrip array antenna for WiFi-5/6 routers. *International Journal of RF and Microwave Computer-Aided Engineering* **2023**(1), 6640730.
5. **Muttair KS, Ghazi Zahid AZ, Shareef OA, Qasim Kamil AM and Mosleh MF** (2022) A novel design of wide and multi-bands 2×2 multiple-input multiple-output antenna for 5G mm-wave applications. *International Journal of Electrical & Computer Engineering* **12**(4), 3882–3890.
6. **Sakli H, Abdelhamid C, Essid C and Sakli N** (2021) Metamaterial-based antenna performance enhancement for MIMO system applications. *IEEE Access* **9**, 38546–38556.
7. **Muttair KS, Aljawaheri KK, Ali MZ, Shareef OA and Mosleh MF** (2022) New ultra-small design and high performance of an 8×8 massive MIMO antenna for future 6G wireless devices. *Indonesian Journal of Electrical Engineering and Computer Science* **28**(1), 587–599.
8. **Paul LC, Hye SA, Rani T, Hossain MI, Karaaslan M, Ghosh P and Saha HK** (2023) A compact wrench-shaped patch antenna with a slotted parasitic element and semi-circular ground plane for 5G communication. *e-Prime-Advances in Electrical Engineering, Electronics, and Energy* **6**, 100334.
9. **Huang H-C** (2018) Overview of antenna designs and considerations in 5G cellular phones. In *2018 International Workshop on Antenna Technology (iWAT)*, 1–4. IEEE.
10. **Muttair KS, Shareef OA and Mosleh MF** (2023) High performance MIMO array antenna for 5G systems. *International Journal of Microwave & Optical Technology* **18**(5), 529–539.
11. **Bariah L, Mohjazi L, Muhaidat S, Sofotasios PC, Kurt GK, Yanikomeroglu H and Dobre OA** (2020) A prospective look: Key enabling technologies, applications, and open research topics in 6G networks. *IEEE Access* **8**, 174792–174820.
12. **Rajatheva N, Atzeni I, Bjornson E, Bourdoux A, Buzzi S, Dore J-B, Erkucuk S, Fuentes, M., Guan, K., Hu, Y and Huang, X.** (2020) White paper on broadband connectivity in 6G. *arXiv preprint arXiv:2004.14247*, 1–46.
13. **Ibrahim SK, Jit Singh M, Al-Bawri SS, Ibrahim HH, Islam MT, Islam MS, Alzamil A and Abdulkawi WM** (2023) Design, challenges, and developments for 5G massive MIMO antenna systems at sub-6-GHz band: A review. *Nanomaterials* **13**(3), 520.
14. **Usha Sharma and Garima Srivastava** (2020) A study of various techniques to reduce mutual coupling in MIMO antennas. In *2020 Second International Conference on Inventive Research in Computing Applications (ICIRCA)*, 1–7. IEEE.
15. **Sharma U, Srivastava G and Khandelwal MK** (2021) A compact wide impedance bandwidth MIMO antenna with vias and parasitic strip. In *2021 IEEE Madras Section Conference (MASCON)*, 1–4. IEEE.
16. **Sharma U, Srivastava G and Khandelwal MK** (2021) Small MIMO antenna with circular polarization for UHF RFID, PCS, and 5G applications. In *2021 IEEE International Conference on RFID Technology and Applications (RFID-TA)*, 223-226.
17. **Rahman I, Razavi SM, Liberg O, Hoymann C, Wiemann H, Tidestav C, Schliwa-Bertling P, Persson P and Gerstenberger D** (2021) 5G evolution toward 5G advanced: An overview of 3GPP releases 17 and 18. *Ericsson Technology Review* **2021**(14), 2–12.
18. **Muttair KS, Shareef OA, Mosleh MF, Ghazi Zahid AZ, Shakir AM and Qasim AM** (2023) A dual-element quad-port MIMO antenna modern design with ideal isolation correlation for 5G systems. In *AIP Conference Proceedings*, **2804**(1), 1–11. AIP Publishing.
19. **Tiwari RN, Singh P, Kumar P and Kanaujia BK** (2022) High isolation 4-port UWB MIMO antenna with novel decoupling structure for high speed and 5G communication. In *2022 International Conference on Electromagnetics in Advanced Applications (ICEAA)*, 336–339. IEEE.
20. **Muttair KS, Shareef OA and Taher HB** (2023) Novel fractal geometry of 4×4 multi-input and multi-output array antenna for 6G wireless systems. *TELKOMNIKA (Telecommunication Computing Electronics and Control)* **22**(1), 17–25.
21. **Khalid M, Syeda IN, Niamat H, Rahman M, Fawad Y, Mirjavadi SS, Khan MJ and Amin Y** (2020) 4-port MIMO antenna with defected ground structure for 5G millimeter-wave applications. *Electronics* **9**(1), 71.
22. **Pei T, Zhu L, Wang J and Wen W** (2021) A low-profile decoupling structure for mutual coupling suppression in MIMO patch antenna. *IEEE Transactions on Antennas and Propagation* **69**(10), 6145–6153.
23. **Kiani SH, Savci HS, Munir ME, Sedik A and Mostafa H** (2023) An ultra-wide band MIMO antenna system with enhanced isolation for microwave imaging applications. *Micromachines* **14**(9), 1732.
24. **Arshad F, Ahmad A, Amin Y, Babar Abbasi MA and Choi D-Y** (2022) MIMO antenna array with the capability of dual polarization reconfiguration for 5G mm-wave communication. *Scientific Reports* **12**(1), 18298.
25. **Elabd RH** (2023) Compact dual-port MIMO filtering-based DMS with high isolation for C-band and X-band applications. *EURASIP Journal on Wireless Communications and Networking* **2023**(1), 110.
26. **Megahed AA, Abdelhay EH, Abdelazim M and Soliman HYM** (2023) 5G millimeter-wave wideband MIMO antenna arrays with high isolation. *EURASIP Journal on Wireless Communications and Networking* **61**(1), 1–16.
27. **Yanhong X, Dong P, Wang A, Hou J and Shanshan L** (2024) A quad-band high-isolated MIMO microstrip antenna for coal mine communication. *Progress in Electromagnetics Research Letters* **115**, 39–46.

28. **Ali A, Munir ME, Marey M, Mostafa H, Zakaria Z, Abdullah Al-Gburi AJ and Bhatti FA** (2023) A compact MIMO multiband antenna for 5G/WLAN/WIFI-6 devices. *Micromachines* **14**(6), 1153.
29. **Lina M, Shao Z, Lai J, Changzhan G and Mao J** (2024) Bandwidth enhancement of H-plane MIMO patch antennas in integrated sensing and communication applications. *IEEE Open Journal of Antennas and Propagation* **5**(1), 90–103.
30. **Lavadiya S, Sorathiya V and Patel SK** (2023) 1×2 printed element-based MIMO antenna with UWB and multiband response for air-borne and naval radar communication. *In Terahertz, RF, Millimeter, and Submillimeter-Wave Technology and Applications XVI* 12420, 119–127. SPIE.
31. **Tighilt Y, Bensid C, Sayad D, Mekki S, Zegadi R, Bouknia ML, Elfergani I, Singh P, Rodriguez J and Zebiri C** (2023) Low-profile UWB-MIMO antenna system with enhanced isolation using parasitic elements and metamaterial integration. *Electronics* **12**(23), 4852.
32. **Sharma A, Gupta SK, Mark R, Shukla B and Das S** (2023) Resistance loaded UWB MIMO with enhanced isolation for S and C band applications. *Progress in Electromagnetics Research C* **134**, 197–209.
33. **Roges R, Malik PK, Sharma S, Arora SK and Maniraguha F** (2023) A miniaturized, dual-port, multiband MIMO with CSRR DGS for internet of things using WLAN communication standards. *Wireless Communications and Mobile Computing* **2023**, 1–21.
34. **Khan I, Zhang K, Qun W, Ullah I, Ali L, Ullah H and Ur Rahman S** (2022) A wideband high-isolation microstrip MIMO circularly-polarized antenna based on the parasitic element. *Materials* **16**(1), 103.
35. **Munusami C and Venkatesan R** (2024) A compact boat shaped dual-band MIMO antenna with enhanced isolation for 5G/WLAN application. *IEEE Access* **12**, 11631–11641.
36. **Tran H-H, The-Lam Nguyen T, Hoai-Nam T and Pham D-P** (2023) A metasurface-based MIMO antenna with compact, wideband, and high isolation characteristics for sub-6 GHz 5G applications. *IEEE Access* **11**, 67737–67744.
37. **You X, Du C and Yang Z-P** (2023) A flexible CPW 2-port dual notched-band UWB-MIMO antenna for wearable IoT applications. *Progress in Electromagnetics Research C* **128**, 155–168.
38. **Kumar P, Kumar Singh A, Kumar R, Mahto SK, Pal P, Sinha R, Choubey A and Al-Gburi AJA** (2024) Design and analysis of low profile stepped feedline with dual circular patch MIMO antenna and stub loaded partial ground plane for wireless applications. *Progress in Electromagnetics Research C* **140**, 135–144.
39. **Kempanna SB, Biradar RC, Kumar P, Kumar P, Pathan S and Ali T** (2023) Characteristic-mode-analysis-based compact vase-shaped two-element UWB MIMO antenna using a unique DGS for wireless communication. *Journal of Sensor and Actuator Networks* **12**(3), 47.
40. **Hossein MR, Ramzan M and Sen P** (2024) Slot-loading based compact wideband monopole antenna design and isolation improvement of MIMO for Wi-Fi sensing application. *Microwave and Optical Technology Letters* **66**(1), e33886.
41. **Wang Z, Ren W, Nie W, Weidong M and Chenlu L** (2023) Design of three-band two-port MIMO antenna for 5G and future 6G applications based on fence-shaped decoupling structure. *Progress in Electromagnetics Research C* **134**, 249–261.
42. **Dwivedi AK, Narayanaswamy NK, Varma Penmatsa KK, Singh SK, Sharma A and Singh V** (2023) Circularly polarized printed dual port MIMO antenna with polarization diversity optimized by machine learning approach for 5G NR n77/n78 frequency band applications. *Scientific Reports* **13**(1), 13994.
43. **Babu KV, Das S, Ali SS, Ghzaoui MEL, Phani Madhav BT and Patel SK** (2023) Broadband sub-6 GHz flower-shaped MIMO antenna with high isolation using a theory of characteristic mode analysis (TCMA) for 5G NR bands and WLAN applications. *International Journal of Communication Systems* **36**(6), e5442.
44. **Firmansyah T, Praptodiyono S, Permana J, Alam S, Supriyanto T, Paramayudha K, Wahyu Y, Alaydrus M and Kondoh J** (2023) Modeling of quasi-tapered microstrip antenna based on expansion-exponential tapered method and its application for wideband MIMO structure. *AEU-International Journal of Electronics and Communications* **169**, 154745.
45. **Sayeed SS, Pandey A, Singh AK and Kumar A** (2023) Investigation of meandered line and slot loaded techniques based MIMO antenna for 5G (N258) and satellite applications. *Journal of Southwest Jiaotong University* **58**(1), 1363–1381.
46. **Nan J, Pan J, Han X and Wang Y** (2023) Design of a novel superwideband dual port antenna with second-order Hilbert branches and a modified T-decoupling structure. *International Journal of Antennas and Propagation* **2023**, 1–12.
47. **Tiwari P, Gahlaut V, Kaushik M, Shastri A, Siddiqui G and Singh B** (2023) A high-frequency planar-configured millimeter-wave MIMO antenna for fifth-generation NR operations. *International Journal of RF and Microwave Computer-Aided Engineering* **2023**, 1–14.
48. **Aziz RS, Koziel S, Leifsson L and Szczepanski S** (2023) A study of mutual coupling suppression between two closely spaced planar monopole antenna elements for 5G new radio massive MIMO system applications. *Electronics* **12**(12), 2630.
49. **Taher F, Al Hamadi H, Alzaidi MS, Alhumyani H, Elkamchouchi DH, Elkamshoushy YH, Haweel MT, Abo Sree MF and Abdel Fatah SY** (2023) Design and analysis of circular polarized two-port MIMO antennas with various antenna element orientations. *Micromachines* **14**(2), 380.
50. **Tiwari P, Gahlaut V, Kaushik M, Shastri A, Arya V, Elfergani I, Zebiri C and Rodriguez J** (2023) Enhancing the performance of millimeter wave MIMO antenna with a decoupling and common defected ground approach. *Technologies* **11**(5), 142.
51. **Islam T, Alsunaydih FN, Alsaleem F and Alhassoon K** (2023) Analyzing the performance of millimeter wave MIMO antenna under different orientation of unit element. *Micromachines* **14**(11), 1975.
52. **Farooq U and Lokam A** (2023) A compact 26/39 GHz millimeter-wave MIMO antenna design for 5G IoT applications. *Journal of Infrared, Millimeter, and Terahertz Waves* **44**(5), 1–13.
53. **Bisht N, Kumar Malik P, Das S, Islam T, Asha S and Alathbah M** (2023) Design of a modified MIMO antenna based on tweaked spherical fractal geometry for 5G new radio (NR) band N258 (24.25–27.25 GHz) application. *Fractal and Fractional* **7**(10), 718.
54. **Sghaier N, Belkadi A, Malleh MA, Latrach L, Hassine IB and Gharsallah A** (2024) Design and analysis of a compact MIMO antenna for 5G mmWave N257, N260, and N262 band applications. *Journal of Infrared, Millimeter, and Terahertz Waves* **45**(3), 1–18.
55. **Desai PK and Bindu S** (2023) Design and fabrication of a 2-port multiple antenna system for mmwave application. *Journal of Communications* **18**(11), 705–713.
56. **Jakhar J, Jhajharia T and Gupta B** (2023) Asymmetric flare shape patch MIMO antenna for millimeter wave 5G communication systems. *Progress in Electromagnetics Research C* **136**, 75–86.
57. **Ud Din I, Ullah S, Mufti N, Ullah R, Kamal B and Ullah R** (2023) Metamaterial-based highly isolated MIMO antenna system for 5G smartphone application. *International Journal of Communication Systems* **36**(3), e5392.
58. **Gao M, Niu H, Nan JC, Liu WH and Liu CL** (2023) 2-port high gain millimeter-wave MIMO antenna for 5G applications. *Progress in Electromagnetics Research M* **120**, 15–27.
59. **Ali WAE, Ibrahim AA and Ahmed AE** (2023) Dual-band millimeter wave 2×2 MIMO slot antenna with low mutual coupling for 5G networks. *Wireless Personal Communications* **129**(4), 2959–2976.
60. **Kaur Sidhu A and Singh Sivia J** (2023) Design of wideband fractal MIMO antenna using Minkowski and Koch hybrid curves on half octagonal radiating patch with high isolation and gain for 5G applications. *Advanced Electromagnetics* **12**(1), 58–69.
61. **Sokunbi O, Attia H, Hamza A, Shamim A, Yiyang Y and Kishk A** (2023) New Self-Isolated MIMO Antenna Array for 5G mm-Wave Applications. Authorea Preprints.
62. **Shaik I and Krishna Veni S** (2023) A compact dual-band octal patch loaded with bow-tie parasitic MIMO antenna design for 5G mm-Wave wireless communication. *Progress in Electromagnetics Research C* **133**, 121–134.
63. **Khan D, Ahmad A and Choi D-Y** (2024) Dual-band 5G MIMO antenna with enhanced coupling reduction using metamaterials. *Scientific Reports* **14**(1), 96.

64. **Sehrai DA, Asif M, Khan J, Abdullah M, Shah WA, Alotaibi S and Ullah N** (2022) A high-gain and wideband MIMO antenna for 5G mm-wave-based IoT communication networks. *Applied Sciences* **12**(19), 9530.
65. **Sabek AR, Ali WAE and Ibrahim AA** (2022) Minimally coupled two-element MIMO antenna with dual-band (28/38 GHz) for 5G wireless communications. *Journal of Infrared, Millimeter, and Terahertz Waves* **43**(3-4), 335–348.
66. **Govindan T, Palaniswamy SK, Kanagasabai M and Kumar S** (2022) Design and analysis of UWB MIMO antenna for smart fabric communications. *International Journal of Antennas and Propagation* **2022**, 1–14.
67. **Ibrahim AA and Abo Sree MF** (2022) UWB MIMO antenna with 4-element, compact size, high isolation, and single band rejection for high-speed wireless networks. *Wireless Networks* **28**(7), 3143–3155.
68. **Hasan MM, Islam MT, Abdul Rahim SK, Alam T, Rmili H, Alzamil A, Islam MS and Soliman MS** (2023) A compact Mu-near-zero metamaterial integrated wideband high-gain MIMO antenna for 5G new radio applications. *Materials* **16**(4), 1751.
69. **Alharbi AG, Rafique U, Ullah S, Khan S, Abbas SM, Ali EM, Alibakhshikenari M and Dalarsson M** (2022) Novel MIMO antenna system for ultra-wideband applications. *Applied Sciences* **12**(7), 3684.
70. **Sharaf MH, Zaki AI, Hamad RK and Omar MMM** (2022) A multi-band MIMO antenna system with coupled-fed modified rectangular patch elements for 5G systems. *Advances in Computing and Engineering* **2**(2), 43–59.
71. **Hüseyin Şerif Savcı** (2023) A four element stringray-shaped MIMO antenna system for UWB applications. *Micromachines* **14**(10), 1944.
72. **Shi C, Zhao Z and Chengzhu D** (2023) A design of quad-element dual-band MIMO antenna for 5G application. *Micromachines* **14**(7), 1316.
73. **Sarkar GA, Parvez KM, Ambika A, Islam T, Das S, Mandal U and Parui SK** (2024) A quad port MIMO antenna using rectangular dielectric resonator antenna array for intelligent transportation system applications. *Progress in Electromagnetics Research M* **123**, 45–52.
74. **Babu SR and Dinesha PG** (2023) Design and development of sextuple band reject UWB-MIMO antenna for wireless applications. *Progress in Electromagnetics Research C* **128**, 231–246.
75. **Khan O, Khan S, Khan Marwat SN, Gohar N, Bilal M and Dalarsson M** (2023) A novel densely packed 4×4 MIMO antenna design for UWB wireless applications. *Sensors* **23**(21), 8888.
76. **Lin X, Huang G and Zhang Y** (2023) An ultra-wideband MIMO antenna based on dual-mode transmission line feeding for wireless communication. *Progress in Electromagnetics Research M* **122**, 73–83.
77. **Ruihua M, Huang H, Xiaoping L and Wang X** (2023) Triple-band MIMO antenna with integrated decoupling technology. *International Journal of Antennas and Propagation* **2023**, 1–14.
78. **Din Ud I, Alibakhshikenari M, Virdee BS, Ullah S, Ullah S, Akram MR, Mansoor Ali S, Livreri P and Limiti E** (2023) High-performance antenna system in MIMO configuration for 5G wireless communications over sub-6 GHz spectrum. *Radio Science* **58**(10), 1–22.
79. **Aiting W, Tao Y, Zhang P, Zhang Z and Fang Z** (2023) A compact high-isolation four-element MIMO antenna with asymptote-shaped structure. *Sensors* **23**(5), 2484.
80. **Santhikiran B and Kavitha T** (2023) UWB microstrip fed 4-element MIMO antenna for 5G applications. *International Journal of Intelligent Systems and Applications in Engineering* **11**(9s), 342–350.
81. **Kolangiammal S, Balaji L and Mahdal M** (2023) A compact planar monopole UWB MIMO antenna for short-range indoor applications. *Sensors* **23**(9), 4225.
82. **Abbas A, Hussain N, Sufian MA, Awan WA, Jung J, Lee SM and Kim N** (2023) Highly selective multiple-notched UWB-MIMO antenna with low correlation using an innovative parasitic decoupling structure. *Engineering Science and Technology, International Journal* **43**, 101440.
83. **Singh G, Kumar S, Abrol A, Kanaujia BK, Pandey VK, Marey M and Mostafa H** (2023) Frequency reconfigurable quad-element MIMO antenna with improved isolation for 5G systems. *Electronics* **12**(4), 796.
84. **Saxena G, Gupta U, Shukla S, Shukla U, Bharti S, Awasthi YK, Sanjay C, Mohammed Saif WA and Singh H** (2023) High isolation quad-element SWB-MIMO antenna with dual band-notch for ISM and WLAN band wireless applications. *Advanced Electromagnetics* **12**(3), 54–60.
85. **Sereddy CR and Yalavarthi UD** (2023) Star shaped fractal conformal MIMO antenna for WLAN, vehicular and satellite applications. *Progress in Electromagnetics Research M* **119**, 37–50.
86. **Suresh AC, Reddy TS, Phani Madhav BT, Alshathri S, El-Shafai W, Das S and Sorathiya V** (2023) A novel design of spike-shaped miniaturized 4×4 MIMO antenna for wireless UWB network applications using characteristic mode analysis. *Micromachines* **14**(3), 612.
87. **Murugan C and Kavitha T** (2023) A compact four-element modified annular ring antenna for 5G applications. *Progress in Electromagnetics Research C* **137**, 169–183.
88. **Suresh AC and Reddy TS** (2023) Experimental Investigation of novel frock-shaped miniaturized 4×4 UWB MIMO antenna using characteristic mode analysis. *Progress in Electromagnetics Research B* **101**, 45–61.
89. **Sengar S, Malik PK, Srivastava PC, Srivastava K and Gehlot A** (2023) Performance analysis of MIMO antenna design with high isolation techniques for 5G wireless systems. *International Journal of Antennas and Propagation* **2023**, 1–23.
90. **Ramyasree G and Suman N** (2023) Dual-band 4-port Vivaldi MIMO antenna for 5G mmWave applications at 28/39 GHz. *Progress in Electromagnetics Research M* **119**, 13–24.
91. **Aboualalaa M and Mansour I** (2023) Dual-band end-fire four-element MIMO antenna array using split-ring structure for mm-wave 5G applications. *IEEE Access* **11**, 57383-57390.
92. **Munir ME, Hassan Kiani S, Savci HS, Marey M, Khan J, Mostafa H and Parchin NO** (2023) A four-element mm-wave MIMO antenna system with wide-band and high isolation characteristics for 5G applications. *Micromachines* **14**(4), 776.
93. **Güler C and Bayer Keskin SE** (2023) A novel high isolation 4-port compact MIMO antenna with DGS for 5G applications. *Micromachines* **14**(7), 1309.
94. **Abbas MA, Allam A, Gaafar A, Elhennawy HM and Abo Sree MF** (2023) Compact UWB MIMO antenna for 5G millimeter-wave applications. *Sensors* **23**(5), 2702.
95. **Mistri RK, Mahto SK, Singh AK, Sinha R, Abdullah Al-Gburi AJ, Alghamdi TAH and Alathbah M** (2023) Quad element MIMO antenna for C, X, Ku, and Ka-band applications. *Sensors* **23**(20), 8563.
96. **Elsharkawy RR, Hussein KFA and Farahat AE** (2023) Dual-band (28/38 GHz) compact MIMO antenna system for millimeter-wave applications. *Journal of Infrared, Millimeter, and Terahertz Waves* **44**(11), 1016–1037.
97. **Munir ME, Hassan Kiani S, Serif Savci H, Sehrai DA, Muhammad F, Ali A, Mostafa H and Ojaroudi Parchin N** (2023) mmWave polarization diversity wideband multiple-input/multiple-output antenna system with symmetrical geometry for future compact devices. *Symmetry* **15**(9), 1641.
98. **Ud Din I, Alibakhshikenari M, Virdee BS, Rajaguru Jayanthi RK, Ullah S, Khan S, See CH, Golunski L and Koziel S** (2023) Frequency-selective surface-based MIMO antenna array for 5G millimeter-wave applications. *Sensors* **23**(15), 7009.
99. **Kumar A, Kumar A and Kumar A** (2023) Defected ground structure based high gain, wideband and high diversity performance quad-element MIMO antenna array for 5G millimeter-wave communication. *Progress in Electromagnetics Research B* **101**, 1–16.
100. **Parveez Shariff BG, Anil Naik A, Ali T, Mane PR, David RM, Pathan S and Anguera J** (2023) High-isolation wide-band four-element MIMO antenna covering Ka-Band for 5G wireless applications. *IEEE Access* **11**, 123030–123046.
101. **Tadesse AD, Acharya OP and Sahu S** (2022) A compact planar four-port MIMO antenna for 28/38 GHz millimeter-wave 5G applications. *Advanced Electromagnetics* **11**(3), 16–25.
102. **Sufian MA, Hussain N and Kim N** (2023) Quasi-binomial series-fed array for performance improvement of millimeter-wave antenna for 5G MIMO applications. *Engineering Science and Technology, an International Journal* **47**, 101548.
103. **Patel A, Desai A, Elfergani I, Vala A, Mewada H, Mahant K, Patel S, Zebiri C, Rodriguez J and Ali E** (2022) UWB CPW fed 4-port connected ground MIMO antenna for sub-millimeter-wave 5G applications. *Alexandria Engineering Journal* **61**(9), 6645–6658.
104. **Khan MA, Al Harbi AG, Kiani SH, Nordin AN, Munir ME, Saeed SI, Iqbal J, Esraa Mousa A, Alibakhshikenari M and Dalarsson M** (2022)


https://doi.org/10.1017/S1759078724001004 Published online by Cambridge University Press

mmWave four-element MIMO antenna for future 5G systems. *Applied Sciences* **12**(9), 4280.
105. **Ali A, Munir ME, Nasralla MM, Esmail MA, Abdullah Al-Gburi AJ and Bhatti FA** (2024) Design process of a compact tri-band MIMO antenna with wideband characteristics for sub-6 GHz, Ku-band, and millimeter-wave applications. *Ain Shams Engineering Journal* **15**(3), 102579.
106. **Patel AV, Desai A, Elfergani IT, Mewada H, Zebiri C, Mahant K, Rodriguez J and Abd-Alhameed RA** (2023) Computer modelling of compact 28/38 GHz dual-band antenna for millimeter-wave 5G applications. *Computer Modeling in Engineering and Sciences* **137**(3), 2867–2879.
107. **Ibrahim AA, Ali WAE, Alathbah M and Sabek AR** (2023) Four-port 38 GHz MIMO antenna with high gain and isolation for 5G wireless networks. *Sensors* **23**(7), 3557.
108. **Hussain SA, Taher F, Alzaidi MS, Hussain I, Ghoniem RM, Abo Sree MF and Lalbakhsh A** (2023) Wideband, high-gain, and compact four-port MIMO antenna for future 5G devices operating over Ka-band spectrum. *Applied Sciences* **13**(7), 4380.
109. **Kumar S, Raheja DK, Palaniswamy SK, Kanaujia BK, Mostafa H, Choi HC and Kim KW** (2023) Design and implementation of a planar MIMO antenna for spectrum-sensing applications. *Electronics* **12**(15), 3311.
110. **Alassawi SA, Ali WAE, Ismail N and Rizk MRM** (2023) Compact elliptic ring 2×2 and 4×4 MIMO-UWB antenna at 60 GHz for 5G mobile communications applications. *Microsystem Technologies* **29**(4), 431–440.
111. **Elsharkawy RR, Hussein KFA and Farahat AE** (2024) Miniaturized multi-band millimeter-wave Vivaldi antenna with performance optimization at 28 GHz for 5G MIMO applications. *Journal of Infrared, Millimeter, and Terahertz Waves* **45**(3), 208–232.
112. **Hussain M, Mousa Ali E, Rizvi Jarchavi SM, Zaidi A, Imran Najam A, Alotaibi AA, Althobaiti A and Ghoneim SSM** (2022) Design and characterization of a compact broadband antenna and its MIMO configuration for 28 GHz 5G applications. *Electronics* **11**(4), 523.
113. **Raheel K, Altaf A, Waheed A, Kiani SH, Sehrai DA, Tubbal F and Raad R** (2021) E-shaped H-slotted dual band mmWave antenna for 5G technology. *Electronics* **10**(9), 1019.
114. **Kamal MM, Yang S, Ren X-C, Altaf A, Kiani SH, Anjum MR, Iqbal A, Asif M and Saeed SI** (2021) Infinity shell-shaped MIMO antenna array for mm-wave 5G applications. *Electronics* **10**(2), 165.
115. **Sehrai DA, Asif M, Shoaib N, Ibrar M, Jan S, Alibakhshikenari M, Lalbakhsh A and Limiti E** (2021) Compact quad-element high-isolation wideband MIMO antenna for mm-wave applications. *Electronics* **10**(11), 1300.
116. **El-Hassan MA, Hussein KFA and Farahat AE** (2022) Compact dual-band (28/38 GHz) patch for MIMO antenna system of polarization diversity. *The Applied Computational Electromagnetics Society Journal (ACES)* **37**(6), 716–725.
117. **Farahat AE and Hussein KFA** (2021) Dual-band (28/38 GHz) MIMO antenna system for 5G mobile communications with efficient DoA estimation algorithm in noisy channels. *The Applied Computational Electromagnetics Society Journal (ACES)* **36**(3), 282–294.
118. **Hussain M, Awan WA, Ali EM, Alzaidi MS, Alsharef M, Elkamchouchi DH, Alzahrani A and Abo Sree MF** (2022) Isolation improvement of parasitic element-loaded dual-band MIMO antenna for mm-Wave applications. *Micromachines* **13**(11), 1918.
119. **Sharma S and Arora M** (2022) A millimeter-wave elliptical slot circular patch MIMO antenna for future 5G mobile communication networks. *Progress in Electromagnetics Research M* **110**(13), 235–247.
120. **Jayanthi K and Kalpana AM** (2023) Design of six element MIMO antenna with enhanced gain for 28/38 GHz mm-Wave 5G wireless application. *Computer Systems Science & Engineering* **46**(2), 1689–1705.
121. **Shao R, Chen X, Wang J and Wang X** (2022) Design and analysis of an eight-port dual-polarized high-efficiency shared-radiator MIMO antenna for 5G mobile devices. *Electronics* **11**(10), 1628.
122. **Fawad Y, Ullah S, Irfan M, Ullah R, Rahman S, Muhammad F, Almawgani AHM and Faraj Mursal SN** (2023) Dual-polarized 8-port sub 6 GHz 5G MIMO diamond-ring slot antenna for smartphone and portable wireless applications. *PloS One* **18**(11), e0288793.
123. **Khan MI, Liu S, Mao J, Basit A, Ahmed A and Daraz A** (2023) Electromagnetic coupling suppression of eight-ports MIMO antenna for satellite communication with neutralize block and parasitic elements. *AEU - International Journal of Electronics and Communications* **170**, 154821.
124. **Wang Z, You W, Yang M, Nie W and Weidong M** (2023) Design of MIMO antenna with double L-shaped structure for 5G NR. *Symmetry* **15**(3), 579.
125. **Parchin NO, Mohamed HG, Moussa KH, See CH, Abd-Alhameed RA, Alwadai NM and Amar ASI** (2023) An efficient antenna system with improved radiation for multi-standard/multi-mode 5G cellular communications. *Scientific Reports* **13**(1), 4179.
126. **Abubakar HS, Zhao Z, Kiani SH, Rafique U, Alabdulkreem E and Elmannai H** (2024) Eight element dual-band MIMO array antenna for modern fifth generation mobile phones. *AEU-International Journal of Electronics and Communications* **175**, 155083.
127. **Cholavendan M and Rajeshkumar V** (2024) Dual-feed orthogonally polarized compact 8-element MIMO antenna using metallic stub and decoupling unit for isolation enhancement of sub-6 GHz 5G application. *Progress in Electromagnetics Research Letters* **116**, 105–111.
128. **Sufyan A, Bahadar Khan K, Zhang X, Siddiqui TA and Aziz A** (2024) Dual-band independently tunable 8-element MIMO antenna for 5G smartphones. *Heliyon* **10**, e25712.
129. **Addepalli T, Satish Kumar M, Jetti CR, Gollamudi NK, Kumar BK and Kulkarni J** (2023) Fractal loaded, novel, and compact two-and eight-element high diversity MIMO antenna for 5G sub-6 GHz (N77/N78 and N79) and WLAN applications, verified with TCM analysis. *Electronics* **12**(4), 952.
130. **Morsy MM** (2023) Compact eight-element MIMO antenna array for sub 6 GHz mobile applications. *SN Applied Sciences* **5**(10), 261.
131. **Abubakar HS, Zhao Z, Wang B, Kiani SH, Parchin NO and Hakim B** (2023) Eight-port modified E-slot MIMO antenna array with enhanced isolation for 5G mobile phone. *Electronics* **12**(2), 316.
132. **Guo J, Zhang S, Han C-Z and Zhang L** (2023) Combined open-slot and monopole 8×8 high-isolation broadband MIMO antenna system for sub-6 GHz terminals. *International Journal of Antennas and Propagation* **2023**, 1–14.
133. **Naser HM, Al-Ani OA and Mosleh MF** (2023) W-shaped eight-port wideband MIMO antenna. *Progress In Electromagnetics Research C* **134**, 211–222.
134. **Addepalli T, Manda R, Vidyavathi T, Babu KJ and Kumar BK** (2023) Design of novel compact eight-element lotus shaped UWB-MIMO antenna with triple-notch characteristics on a hollow substrate. *International Journal of Communication Systems* **36**(8), e5465.
135. **Kiani SH, Savci HS, Abubakar HS, Parchin NO, Rimli H and Hakim B** (2023) Eight element MIMO antenna array with tri-band response for modern smartphones. *IEEE Access* **11**, 44244–44253.
136. **Arumugam S and Manoharan S** (2024) Design and performance analysis of 8-port multi-service quad-band MIMO antenna for automotive communication. *International Journal of Numerical Modelling: Electronic Networks, Devices and Fields* **37**(2), e3180.
137. **Song Z, Miao H, Xiaoming X and Wang L** (2023) Design of an enhanced isolation 8-unit MIMO antenna for smartphones operating in 5G nR and LTE 42 bands. *International Journal of Antennas and Propagation* **2023**(1), 7157515.
138. **Huang J, Shen L, Xiao S, Shi X and Liu G** (2023) A miniature eight-port antenna array based on split-ring resonators for 5G sub-6 GHz handset applications. *Sensors* **23**(24), 9734.
139. **Wang Z, Mingzhong L, Yang M, Nie W, Weidong M, Lin H and Zhongyuan L** (2023) Design of wideband 8-element MIMO mobile phone antenna based on sub-6GHz NR band. *Progress in Electromagnetics Research C* **129**, 187–201.
140. **Singh HV, Siva Prasad DV and Tripathi S** (2023) Self-isolated MIMO antenna using mixed-coupling by close coupling technique. *Scientific Reports* **13**(1), 5636.
141. **Kaur I, Basu B and Singh A** (2023) Sub-6 GHz metallic via integrated MIMO antenna array for 5G smartphone. *Progress in Electromagnetics Research C* **138**, 91–104.

142. **Khan A, Yejun H and Chen ZN** (2023) An eight-port circularly polarized wideband MIMO antenna based on a metamaterial-inspired element for 5G mmWave applications. *IEEE Antennas and Wireless Propagation Letters*, **22**(7), 1572-1576.
143. **Zhang Y-M, Yao M and Zhang S** (2023) Wide-band decoupled millimeter-wave antenna array for massive MIMO systems. *IEEE Antennas and Wireless Propagation Letters* **22**(11), 2680–2684.
144. **Babu NS, Ansari AQ, Kumar S, Kanaujia B, Singh G and Goyal B** (2023) Octa-port high gain MIMO antenna backed with EBG for mm-Wave applications. *Progress in Electromagnetics Research B* **103**, 139–157.
145. **Ahmad A and Choi D-Y** (2022) Compact eight-element MIMO antenna with reduced mutual coupling and beam-scanning performance. *Sensors* **22**(22), 8933.
146. **Pramon S, Basuki BS and Syamsul SH** (2019) A compact design eight-element multiple input multiple output millimeter-wave antenna. *Journal of Engineering Science and Technology* **14**(1), 265–278.
147. **Khabba A, Amadid J, Mohapatra S, El Ouadi Z, Ahmad S, Ibnyaich S and Zeroual A** (2022) UWB dual-port self-decoupled o-shaped monopole MIMO antenna with small-size easily extendable design and high diversity performance for millimeter-wave 5G applications. *Applied Physics A* **128**(8), 725.
148. **Musaed AA, Al-Bawri SS, Abdulkawi WM, Aljaloud K, Yusoff Z and Islam MT** (2024) High isolation 16-port massive MIMO antenna-based negative index metamaterial for 5G mm-wave applications. *Scientific Reports* **14**(1), 290.
149. **Liao Y, Cai K, Hubing TH and Wang X** (2014) Equivalent circuit of normal mode helical antennas using frequency-independent lumped elements. *IEEE Transactions on Antennas and Propagation* **62**(11), 5885–5888.
150. **Cheng-Hsun W, Zhou G-T, Yi-Lung W and Tzyh-Ghuang M** (2013) Stub-loaded reactive decoupling network for two-element array using even–odd analysis. *IEEE Antennas and Wireless Propagation Letters* **12**, 452–455.
151. **Papamichael VC and Soras CF** (2009) MIMO antenna modelling using the effective length matrices. *Progress in Electromagnetics Research C* **10**, 111–127.
152. **Verma RK, Priya B, Singh M, Singh P, Yadav A and Singh VK** (2023) Equivalent circuit model-based design and analysis of microstrip line fed electrically small patch antenna for sub-6 GHz 5G applications. *International Journal of Communication Systems* **36**(17), e5595.
153. **Jabire AH, Abana MA, Saminu S, Adamu MJ and Sadiq AM** (2024) Equivalent circuit of a frequency reconfigurable metamaterial MIMO antenna for internet of things applications. *Nigerian Journal of Engineering Science and Technology Research* **10**(1), 51–67.
154. **Kobrin K, Zimeng L, Sledkov V and Manuilov M** (2020) A broadband dual-polarized planar dipole antenna array for sub-6 GHz base stations. In *2020 7th All-Russian Microwave Conference (RMC)*, 180–183.
155. **Naser HM, Al-Ani OA, Muttair KS, Mosleh MF and Taher HB** (2023) Wideband MIMO antenna in the shape of a hand grip. In *2023 International Conference on Smart Applications, Communications and Networking (SmartNets)*, 1–6. IEEE.
156. **Ishteyaq I and Muzaffar K** (2022) Multiple input multiple output (MIMO) and fifth generation (5G): An indispensable technology for sub-6 GHz and millimeter wave future generation mobile terminal applications. *International Journal of Microwave and Wireless Technologies* **14**(7), 932–948.
157. **Muttair KS, Ghazi Zahid AZ, Shareef Al-Ani OA, AL-Asadi AMQ and Mosleh MF** (2021) Antennas performance comparison of multi-bands for optimal outdoor and indoor environments wireless coverage. *Indonesian Journal of Electrical Engineering and Informatics (IJEEI)* **9**(4), 846–858.
158. **Patteti K, Tipparti A and Umamaheshwar S** (2019) Fundamentals and challenges of massive MIMO for 5G. *International Journal of Innovative Technology and Exploring Engineering* **8**(11), 61–65.
159. **Jaglan N, Gupta SD and Sharawi MS** (2021) 18 element massive MIMO/diversity 5G smartphones antenna design for sub-6 GHz LTE bands 42/43 applications. *IEEE Open Journal of Antennas and Propagation* **2**, 533–545.
160. **Sabaawi AMA, Muttair KS, Al-Ani OA and Sultan QH** (2022) Dual-band MIMO antenna with defected ground structure for sub-6 GHz 5G applications. *Progress in Electromagnetics Research C* **122**, 57–66.


**Karrar Shakir Muttair** received a bachelor's degree in Computer Technology Engineering specializing in Communications and Networks from the Islamic University/Iraq in 2016. He worked as a laboratory engineer at the same university until 2017. He completed his M.Sc. in Computer Engineering at Middle Technique University, Baghdad, in 2019. He is currently employed as a lecturer and researcher at the Nanotechnology and Advanced Materials Research Unit, Faculty of Engineering, University of Kufa. He has published various types of research in the field of communications engineering. He is currently teaching and conducting research programs in computer networks and communications. He has received numerous awards and certificates for his outstanding work. His research interests are computer techniques engineering, computer communications networks, multimedia learning, antennas, indoor & outdoor wireless networks, wireless sensor networks, and mobile learning. You can contact him at the following email addresses: karrars.alnomani@uokufa.edu.iq, karraralnomani123@gmail.com, karraralnomani@gmail.com, bbc0078@mtu.edu.iq.

**Oras Ahmed Shareef** received B.Sc. and M.Sc. degrees in Laser and Optoelectronic Engineering from Al-Nahreen University, Iraq, in 2000 and 2002, respectively, and a Ph.D. (2018) in Nanomaterial-based solar cell from Newcastle University, UK. Her research area (within the Emerging Technology and Materials group) is renewable energy, with a research portfolio based on the first-principles simulation of defects and impurities in semiconductors, crystal surfaces, nanostructures, and photovoltaic technologies. Furthermore, her interest lies in communication engineering and related advanced applications, such as indoor and outdoor wave propagation, antenna designs, and applications. Dr. Al-Ani has more than 50 published works in local and international journals, in addition to her participation in several internal and international conferences. Since 2005, Dr. Oras has been a lecturer and an undergraduate supervisor at the College of Electrical Techniques Engineering in Baghdad, Iraq. During her Ph.D. study (2014–2018) at Newcastle University, she had the opportunity to demonstrate and teach in several labs at different levels at the School of Electrical and Electronics Engineering, where she acted as a Teaching Assistant and Lab demonstrator. You can contact her at the following email address: dr.oras@mtu.edu.iq.

**Hazeem Baqir Taher** is a professor at the Department of Computer Science, College of Education for Pure Sciences, Thi-Qar University, Thi-Qar, Iraq. He is also the Director General of the Missions and Cultural Relations in the Iraqi Ministry of Higher Education and Scientific Research. He has a Ph.D. and is interested in working in image processing and intelligence systems. In addition, he published many research papers in his field of specialization. Dr. Hazeem B. Taher has more than 30 published works in local and international journals. His expertise encompasses wireless communications, digital signal processing, image processing, data compression, audio coding, and computer graphics. You can contact him at the following email address: hazecomp792004@gmail.com.

https://doi.org/10.1017/S1759078724001004 Published online by Cambridge University Press